

TURBULENT CONVECTIVE HEAT TRANSFER FROM ROUGH SURFACES WITH TWO-DIMENSIONAL RECTANGULAR RIBS

M. DALLE DONNE† and L. MEYER

Gesellschaft für Kernforschung mbH., INR, Karlsruhe, West Germany

(Received 29 July 1976)

Abstract—Artificial roughness is often used in nuclear reactors to improve the thermal performance of the fuel elements. Although these are made up of clusters of rods, the experiments to measure the heat-transfer and friction coefficients of roughnesses are performed with single rods contained in smooth tubes. The paper illustrates a new transformation method to obtain data applicable to reactor fuel elements from these annulus experiments. New experimental friction data are presented for ten rods, each with a different artificial roughness made up of two-dimensional rectangular ribs. For each rod four tests have been performed, each in a different outer smooth tube. For two of these rods, each for two different outer tubes, heat-transfer data are also given. The friction and heat-transfer data, transformed with the present method, are correlated by simple equations. In the paper, these equations are applied to a case typical for a Gas Cooled Fast Reactor fuel element.

NOMENCLATURE

Geometrical parameters

- A , cross section area of the coolant channel (of a tube, of an annulus, and of the unit cell or subchannel of a rod bundle) [cm²];
 b , width of the roughness rib [cm];
 d , diameter of the rod in a rod bundle [cm];
 D , diameter of the tube [cm];
 D_1 , diameter of the inner cylinder of the annulus [cm];
 D_2 , diameter of the outer cylinder of the annulus [cm];
 D_h , $= \frac{4A}{P}$, hydraulic diameter of the coolant channel [cm];
 h , height of the roughness ribs [cm];
 h_s , height of the Nikuradse sand roughness [cm];
 p , axial pitch of the repeated roughness ribs [cm];
 p_r , pitch of the rods in a rod bundle [cm];
 P , wetted perimeter of a coolant channel [cm];
 r , radial distance of considered cylindrical surface from the axis of symmetry [cm];
 r_0 , radius of the zero-shear-stress line in an annulus cross section [cm];
 r_1 , mean volumetric radius of the inner rod averaged over total length of the rough surface [cm];
 r_2 , radius of the outer cylinder of the annulus [cm];
 R , tube radius [cm];
 S_1 , outer surface of 10 cm length of the inner tube of the annulus [cm²];
 S_2 , inner surface of 10 cm length of the outer tube of the annulus [cm²];

- α , $= r_1/r_2$;
 β , $= r_0/r_2$;
 x , axial distance parallel to the flow [cm];
 y , radial distance from the wall of the considered point [cm];
 \hat{y} , radial distance between the wall and the surface of zero shear [cm];

Gas properties

- c_p , specific heat at constant pressure [cal/g °C];
 k , thermal conductivity [cal/cm s °C];
 γ , specific heat ratio [dimensionless];
 ν , kinematic viscosity [cm²/s];
 ρ , density [g/cm³].

Temperatures

- T , temperature of the gas at the considered circumference [K];
 T_B , $T - (u_B^2/2 \cdot 10^7 J c_p) =$ absolute static bulk temperature of the gas [K];
 T_E , absolute total gas temperature at the test section entrance = absolute static gas temperature at the entrance (because the gas velocity is very small there) [K];
 T_T , $T_E + (Q_g/Mc_p) =$ absolute total bulk temperature of the gas [K];
 T_W , absolute temperature of the wall of the inner tube [K];
 T_{W_o} , absolute temperature of the wall of the outer tube [K];
 $T_{h/2}$, arithmetic average between the temperature of the rough surface T_W and the temperature for $y = h$, as defined by the logarithmic temperature profile [K];
 T_1 , gas bulk temperature of the inner region of the annulus [K];
 T_2 , gas bulk temperature of the outer region of the annulus [K].

†Euratom, delegated to The Karlsruhe "Fast Breeder Project", Institut für Neutronenphysik und Reaktortechnik.

Other physical parameters

- h , convective heat-transfer coefficient between inner tube surface and gas bulk [cal/cm² s °C];
- J , conversion factor from heat units to work units = 4.187 [W s/cal];
- M , mass flow rate of gas [g/s];
- p , absolute static pressure of the gas [dyne/cm²];
- Q_g , quantity of heat given to gas from entrance to the considered cross section of the annulus [cal/s];
- q , heat flux [cal/cm² s];
- q_{e1} , heat produced by Joule effect in a segment equal to 10 cm in length of the inner tube [cal/s];
- q_{g1} , heat given to gas in 10 cm length of the test section [cal/s];
- q_{g1} , heat given to gas directly by the inner tube in 10 cm length of the test section [cal/s];
- q_{g2} , heat given to gas by the outer tube in 10 cm length of the test section [cal/s];
- q_1 , heat lost radially by conduction through insulation for 10 cm length of test section [cal/s];
- q_r , heat transmitted radially by radiation from inner tube to outer tube for 10 cm length of test section [cal/s];
- q'_{g1} , heat given to gas directly by inner tube per unit surface [cal/cm² s];
- q'_{g2} , heat given to gas directly by outer tube per unit surface [cal/cm² s];
- u , velocity of the gas [cm/s];
- u_B , = $M/A\rho_B$, velocity of the bulk of the gas [cm/s]; for constant c_p : $u_B = \bar{u}$;
- u_{\max} , velocity for $r = r_0$ [cm/s];
- u_1 , velocity of the bulk of the gas in the inner region of annulus [cm/s];
- u_2 , velocity of the bulk of the gas in the outer region of annulus [cm/s];
- \bar{u} , average velocity of the gas in a section [cm/s];
- u^* , $(\tau/\rho)^{1/2}$, friction velocity [cm/s];
- ϵ_1 , total emissivity of the outer surface of inner tube [dimensionless];
- ϵ_2 , total emissivity of the inner surface of the outer tube [dimensionless];
- ϵ_{12} , = $\frac{1}{1/\epsilon_1 + S_1/S_2(1/\epsilon_2 - 1)}$ [dimensionless];
- σ , Stefan-Boltzmann constant [cal/cm² s K⁴];
- τ , shear stress at the wall [dyne/cm²];
- ϵ_H , average heat eddy diffusivity of the gas in turbulent flow [cm²/s];
- ϵ_M , average momentum eddy diffusivity of the gas in turbulent flow [cm²/s].

Dimensionless groups

- A_H , slope of the logarithmic temperature profile relative to a rough surface;

- A_M , slope of the logarithmic velocity profile relative to a rough surface;
- A_S , slope of the logarithmic velocity profile relative to a smooth surface;
- f , = $2\tau/\rho_B u_B^2$, friction coefficient (or friction factor) evaluated at the gas bulk temperature T_B ;
- f_0 , friction factor for circular smooth pipes (from Prandtl-Nikuradse universal law of friction for smooth pipes);
- $G(h^+, Pr)$, = $G(h^+)$ for gases, function of Dipprey and Sabersky inversely proportional to the roughness cavity Stanton number;
- $G(h^+)^*$, value of $G(h^+)$ defined by equation (58);
- h^+ , = $\frac{hu^*}{v_B} = \frac{h}{D_h} Re \left(\frac{f_R}{2} \right)^{1/2}$, dimensionless height of roughness ribs, roughness cavity Reynolds number;
- h_w^+ , = $\frac{hu^*}{v_w} = \frac{h}{D_h} Re_w \left(\frac{f_R}{2} \right)^{1/2}$, dimensionless height of roughness ribs evaluated at the wall temperature T_w , roughness cavity Reynolds number evaluated at the wall temperature T_w ;
- Ma , = $u_B/(\gamma p/\rho_B)^{1/2}$, Mach number evaluated at the gas bulk temperature T_B ;
- Nu , = hD_h/k_B , Nusselt number evaluated at the gas bulk temperature T_B ;
- Pr , = $\frac{v_B \rho_B c_{pB}}{k_B}$, Prandtl number evaluated at the gas bulk temperature T_B ;
- Re , = $u_B D_h/v_B$, Reynolds number evaluated at the gas bulk temperature T_B ;
- Pr_r , = $\frac{\epsilon_M}{\epsilon_H}$, turbulent Prandtl number;
- Re_w , = $u_B D_h/v_w$, Reynolds number evaluated at the wall temperature T_w ;
- $R(h^+)$, constant in the turbulent velocity distribution of Nikuradse, equal to the gas velocity at the tip of the roughness ribs divided the friction velocity;
- $R'(h^+)$, asymptotic $R(h^+)$ value for small h/\hat{y} values, not affected any more by h/\hat{y} ;
- $R(h^+)_{1\%}$, $R(h^+)$ value for $h/\hat{y} = 0.01$;
- $R(h^+)_{1s}$, = $R(h^+)_{is}$ reduced to the value $T_w/T_B = 1$, i.e. to the isothermal value;
- $R(\infty)$, value of $R(h^+)$ in the region of "fully rough flow", where $R(h^+)$ is quasi constant; in Table 2 it has been calculated as an average of the values for $h_w^+ \geq 70$;
- $R(\infty)_{0.1}$, $R(\infty)$ value reduced to $T_w/T_B = 1$ and $h/\hat{y} = 0.01$;
- St , = $h/\rho_B c_{pB} u_B$, Stanton number evaluated at the gas bulk temperature T_B ;
- t^+ , = $\frac{(T_w - T)\rho_B c_{pB} u^*}{q_g}$, dimensionless gas temperature;

u^+ , = u/u^* , dimensionless gas velocity;
 y^+ , = yu^*/ν_B , dimensionless radial distance from the wall.

Subscripts

No subscripts means generally that the gas physical properties have evaluated at the gas bulk temperature T_b ;

W , gas properties evaluated at the wall temperature T_w ;

1, 2, it refers to the inner and outer regions respectively of an annulus;

max, maximum;

is, isothermal;

R , rough;

S , smooth;

$h/2$, evaluated at the temperature $T_{h/2}$.

1. INTRODUCTION

GASES are not good heat-transfer media, due to their very low density. However, they have been extensively used as coolants in reactors due to their low neutron absorption and low chemical activity. Much effort and ingenuity has been devoted to the improvement of the heat transfer in gas cooled reactors to increase the core power density and thus reduce the electrical power generating costs.

In the commercial gas cooled reactors this improvement has been achieved by means of extended heat-transfer surfaces (Magneox reactors) or by the so-called "artificial roughness" on the surface of the fuel element rods (advanced gas-cooled reactors).

In the high temperature reactors even higher power densities are achieved by means of higher coolant pressures (up to 40–50 atm) and much higher fuel surface temperatures (up to 1000°C) made possible by the adoption of graphite as cladding and structural material.

Gas cooled fast reactors should have power densities in the core two orders of magnitude greater than those present in high temperature reactors [1]. Although a considerable part of this increase is due to the lack of moderator in the reactor, much higher heat-transfer coefficients are still required, especially because the fuel surface temperatures are considerably lower than in HTR's due to the use of metal, and not ceramic, cladding. This is achieved in part with higher gas pressures (pressures up to 80–130 atm have been proposed), in part again by the use of the artificial roughness. This artificial roughness is made up of small ribs at regular intervals on the heat-transfer surface, which act as turbulence promoters breaking up the viscous sublayer in the fluid region nearest to the wall. Both the heat-transfer and the friction losses are increased, but an appropriate figure of merit, St_R^3/f_R —where the Stanton number St_R is a dimensionless number proportional to the heat-transfer coefficient and f_R is the friction factor, proportional to the pressure drop—is generally greater for a "rough" surface than for a smooth one. The ratio St_R^3/f_R is generally called the "thermal performance" of the roughness [2, 3].

2. PREVIOUS WORK: HEAT TRANSFER AND FRICTION FOR FLOW INSIDE ROUGH TUBES

2.1. Friction for flow inside rough tubes: the Nikuradse sand roughness

Although quite a few works had appeared previously [4–9, 11] the first important work on roughness was published by Nikuradse in 1933 [12]. This and the subsequent work of Schlichting [13] were essentially performed to investigate the problem of the drag exerted by water on the hull of ships. The approach of Nikuradse in his early work is, in our opinion, still the best today.

Nikuradse had found in an earlier work on smooth surfaces [10] that the velocity profile in fluids flowing in turbulent flow in smooth tubes could be described, at a certain distance from the wall of the tube, by a law of the wall based on the Prandtl hypothesis on mixing length and shear stress distribution in turbulent flow. Nikuradse's law of the wall is:

$$u^+ = 2.5 \ln y^+ + 5.5 \quad \text{for } y^+ \geq 70. \quad (1)$$

For flow inside tubes having a certain sand roughness on the surface, Nikuradse found that the dimensionless velocity distribution normal to the wall is given by:

$$u^+ = 2.5 \ln (y/h) + R(h^+) \quad (2)$$

which can also be written as:

$$u^+ = 2.5 \ln (y^+/h^+) + R(h^+) \\ = 2.5 \ln y^+ - 2.5 \ln h^+ + R(h^+) \quad (3)$$

i.e. the fluid velocity in presence of rough walls differs from the velocity in presence of smooth walls only by an additive factor, which becomes more important near the wall and is characteristic of the "microscopic geometry" of the roughness. With microscopic geometry of the roughness, we mean the geometrical parameters which define a particular roughness, such as for instance height, width, pitch and form of a transversal-rib-type of roughness, in contrast to macroscopic geometry which is meant to be the general shape of the surface in contact with the fluid (tube, flat plate, annulus, rod bundle, rectangular channel etc.).

The physical meaning of h^+ and $R(h^+)$ is quite clear. h^+ is the Reynolds number based on the height of the roughness and on the friction velocity [$u^* = (\tau/\rho)^{1/2}$] and $R(h^+)$ is the dimensionless flow velocity (related to the friction velocity) at the tip of the roughness.

Nikuradse showed also that:

$$\text{for } 0 < h^+ \leq 5 \quad R(h^+) - 2.5 \ln h^+ = 5.5 \quad (4)$$

and equation (2) reduces to equation (1) valid for an hydraulically smooth regime;

for $h^+ \geq 70$ $R(h^+) = 8.5$ (completely rough regime) (5)

and for $5 < h^+ < 70$ $R(h^+)$ varies with h^+ (transition regime between the completely rough regime and the hydraulically smooth regime).

By integrating equation (2) over y in the cross section of a tube, one has:

$$\bar{u}^+ = u^+_{\max} - 3.75 \quad (6)$$

and noting that

$$\bar{u}^+ = u/u^* = \left(\frac{2}{f_R} \frac{\tau}{\rho}\right)^{\frac{1}{2}} / \left(\frac{\tau}{\rho}\right)^{\frac{1}{2}} = \left(\frac{2}{f_R}\right)^{\frac{1}{2}} \quad (7)$$

and

$$u_{\max}^+ = 2.5 \ln \frac{R}{h} + R(h^+) \quad (8)$$

one obtains the friction factor for the flow in a rough tube, i.e. the so called friction similarity law of Nikuradse:

$$\left(\frac{2}{f_R}\right)^{\frac{1}{2}} = 2.5 \ln \frac{R}{h} + R(h^+) - 3.75. \quad (9)$$

Nikuradse's roughness was geometrically defined by the height of the roughness grain only, because the grains of sand were glued to the wall as closely to each other as possible. Other types of roughness are defined by a greater number of geometrical parameters.

Schlichting [13] measured the friction factors of various roughnesses in rectangular ducts. To characterize the roughness he used the equivalent sand roughness, that is the ratio h_s/R of the Nikuradse sand roughness which gives a friction factor equal to that of the considered roughness. In a completely rough regime, one has from equations (5) and (9):

$$2.5 \ln \frac{R}{h} + R(h^+) = 2.5 \ln \frac{R}{h_s} + 8.5. \quad (10)$$

In present treatment we will use the parameter $R(h^+)$ to characterize a roughness, rather than the equivalent sand roughness h_s/R , because from $R(h^+)$ one can obtain velocity distribution and friction coefficient, while the relationship between $R(h^+)$ and h_s/R is not always so simple as indicated in equation (10). (For instance in the transition regime.)

The method of Nikuradse to correlate its experimental data implied that the parameter $R(h^+)$ of equation (2) is independent of the macroscopic geometry and it is only dependent on type of roughness present on the surface (microscopic geometry).

Schlichting (see chapters 20 and 21 of [14]) showed that equations (1) and (2) are valid with good approximation for other macroscopic geometries besides the pipes, such as rectangular ducts or flat plates, at least not very far from the wall in this second case. This method therefore has the advantage, against the mere use of the friction factor, to separate the effects of the roughness itself from the effects of the geometry of the surface which delimits the flow of the fluid. Thus for instance measurements in pipes can be extended to flat plates and vice versa by simple integration of equation (2). We shall see later on, that $R(h^+)$ is not really completely independent of macroscopic geometry but we can regard this as a second order effect for now.

*By definition $f_R = \tau / \left(\frac{\rho \bar{u}^2}{2}\right)$, therefore: $\bar{u} = \left(\frac{2}{f_R} \frac{\tau}{\rho}\right)^{\frac{1}{2}}$.

2.2. Heat transfer for flow inside rough tubes: the

Dipprey-Sabersky method

Among the first experimental investigations on heat transfer for flow inside artificially rough tubes we should like to mention those of Chu and Streeter in 1949 [15], of Sams [16] and of Nunner [17]. These data were given in terms of friction factors and Nusselt or Stanton numbers.

In 1963 Dipprey and Sabersky published experimental friction and heat-transfer data, which they obtained for flow inside a tube with sand roughness surface [18]. Their method of correlating the heat-transfer results was similar to that used by Nikuradse to correlate the friction data. Although they do not state so explicitly, the main hypothesis of Dipprey and Sabersky is to assume that the dimensionless temperature distribution normal to the rough wall of the tube is given by:

$$t^+ = 2.5 \ln (y/h) + G(h^+, Pr) \quad (11)$$

whereby by definition:

$$t^+ = \frac{(T_W - T) \rho_B c_{pB} u^*}{q'_g} \quad (12)$$

and T_W is the temperature of the rough surface; T is the temperature of the gas at the point distant y from the wall; c_{pB} is the average specific heat at constant pressure of the gas; ρ_B is average gas density; $u^* = (\tau/\rho_B)^{\frac{1}{2}}$ = friction velocity; and q'_g is the heat flux from the rough surface to the gas. That is, the temperature profile in a cross section of a rough tube is assumed to be similar to the dimensionless velocity distribution of Nikuradse for a rough tube [equation (2)].

The integration of equation (11) over y in the cross section of the tubes yields:

$$i^+ = 2.5 \ln \frac{R}{h} + G(h^+, Pr) - 3.75 \quad (13)$$

and where one considers that in analogy to the velocity [see equation (7)]:

$$i^+ = \frac{(f_R/2)^{\frac{1}{2}}}{St_R} \quad (14)$$

one obtains:

$$\frac{(f_R/2)^{\frac{1}{2}}}{St_R} = 2.5 \ln \frac{R}{h} + G(h^+, Pr) - 3.75 \quad (15)$$

analogous to friction similarity law of Nikuradse [equation (9)]. From equation (9) and (15) one obtains the Dipprey and Sabersky equation:

$$G(h^+, Pr) = R(h^+) + \frac{\frac{f_R}{2} - 1}{(f_R/2)^{\frac{1}{2}}}. \quad (16)$$

The data of Dipprey and Sabersky for various Prandtl numbers and three different sand roughnesses were correlated quite well by the parameter $G(h^+, Pr)$. Accordingly, the experimental task of determining the heat-transfer coefficient, i.e. the Stanton number St_R , is now reduced to that of obtaining the function

$G(h^+, Pr)$, which depends on the two variables, h^+ , dimensionless height of the roughness, and the Prandtl number of the fluid. Without this analysis St_R had to be regarded, for geometrically similar roughnesses, as a function of the three parameters h/D , Pr , Re . This simplification is analogous to the one which was made possible by the friction law in connection with the determination of f . Also implicit in this approach is that $G(h^+, Pr)$ is a function of the microscopic geometry of the roughness only and that integration of equation (11) can yield Stanton numbers for other macroscopic geometries as well.

Dipprey and Sabersky speculated that "the rough wall can be imagined to consist of a series of small cavities of depth h and that the time-mean flow in and about these cavities consists of a pattern of one or more standing vortices". For the fully rough flow regime they neglected the viscosity dependent shear stress acting on the wall, which is much smaller than the integrated axial component of the pressure forces on the roughness cavity walls, and showed that the function $G(h^+, Pr)$ is inversely proportional to the cavity Stanton number. They assumed that the flow between the roughness elements consisted of small vortices and that the Stanton number for any of the short boundary layers in the cavity between the roughness elements could be expressed approximately by a relation of the type:

$$St_{vi} = k_{vi} Re_{vi}^{-p} Pr^{-q} \quad (17)$$

where the subscript vi refers to the i th vortex in the cavity. By combining the effects of the different boundary-layer segments they finally arrived at the relation:

$$G(h^+, Pr) = Kh^+{}^p Pr^q \quad (18)$$

where K should have the same value for all the roughnesses geometrically similar (same form, equal p/h and h/b) and p and q should be universal constants. From their own experiments with sand roughness K was found to be equal to 5.19, p and q to 0.20 and 0.44 respectively.

3. HEAT TRANSFER AND FRICTION FOR FLOW INSIDE ANNULI: THE TRANSFORMATION METHOD

3.1. The Hall transformation

The fuel elements of a gas cooled reactor, both thermal or fast are formed by clusters of rods, which are, in part or completely, provided with artificially rough surfaces. The walls of the subassembly shroud which contains the fuel pins are of course always smooth.

Heat-transfer experiments with these fuel elements or fuel elements models, however, take a long time and are very expensive. Furthermore, the experimental data for these complicated geometries are difficult to interpret and to generalize. The experiments are therefore generally performed either with flow inside rough tubes, or with a single rough rod, where heat is generated electrically by Joule effect, contained in a smooth tube thermally insulated from the ambient.

Machining of roughnesses inside a long pipe is very difficult, therefore only a limited number of experiments with sand roughness or simple regular (or artificial) roughness has been performed. The most important of these have been examined in detail in the previous section. Much more frequent are experiments of the second type, called shortly experiments in annuli.

The problem of transforming the friction and heat-transfer data obtained by annuli experiments to fuel element geometries, where the ratio between rough and smooth surface areas, and between areas of the surfaces transmitting heat and adiabatic is quite different from that of an annulus, was originally tackled by Hall [19]. He assumed that the annular space of the cross section of the annulus could be divided into two regions, the inner affected by the inner rough rod, the outer by the smooth surface of the channel. The division line was given by the line of zero shear stress. Hall assumed that this line was coincident with the line of maximum velocity, although this is not always true for turbulent flow, as we shall discuss later. Once the velocity distribution in the annulus cross section has been measured, the separation line of the two regions is defined and the friction coefficient of the inner region can be calculated, neglecting the outer surface of the inner region, because at this position the shear stress is assumed to be equal zero. Similarly the Reynolds number of the inner region can be calculated with the hydraulic diameter based on the surface of the inner rod only. Furthermore, assuming that the heat produced in the rod is going into the inner annulus region only—which is equivalent to assume that the line of zero shear stress and the adiabatic line are coincident—it is possible to calculate the hypothetical temperature distribution and the Stanton number of the inner region of the annulus from the measured temperature distribution in the fluid.

In such a way the boundary conditions of an infinite regular array of rough rods or of the flow inside a tube—where the coincidence of the adiabatic line with the line of zero shear stress is actually realized—are simulated. Thus it can be claimed that the experimental data so transformed can be applicable to an infinite regular array of rough rods, or to the central subchannels of a real array, which are generally unaffected by the smooth walls of the shroud containing the subassembly. For instance these transformed data can be used to calculate temperatures and pressures in the fuel subassembly of a gas cooled fast reactor which is formed by a large number of pins in a regular array, at least for the rods not directly adjacent to the subassembly wall.

3.2. The Wilkie transformation

The Hall transformation requires measurements of velocity and temperature profiles in the annulus cross sections. These measurements are long and cumbersome and generally require much bigger test sections than those used for simple friction and heat-transfer measurements. Wilkie therefore proposed a simplified and empirical transformation method based on his

series of measurements of velocity and temperature profiles in annuli with a radius ratio equal to 0.5, with the inner surface roughened by transversal square ribs (in the range $5 \leq p/h \leq 15$, $0.001 \leq h/D_{h1} \leq 0.010$, and $8 \times 10^4 \leq Re_1 \leq 1.3 \times 10^6$) [20]. Using the maximum velocity criterion for separation of the two regions of the annulus, Wilkie found that the ratio of the average flow velocities in the two regions of the annulus is a function of the ratio of the friction factor of the inner rough rod to the friction factor of a smooth pipe at the same Reynolds number (friction factor multiplier). When the friction factor multiplier is greater than five, the velocity ratio is constant and equal to 1.02. Similarly he produced graphs, correlating all his experimental results, giving the mean coolant temperatures on either side of the maximum velocity line as function of the ratio of the temperature of the inner rough surface to the average gas temperature (T_w/T_B) and of the transformed Reynolds number of the inner region of the annulus (Re_1). Finally he obtained the friction factor of the outer smooth surface of the annulus as a function of the outer region Reynolds number and of the inner rough surface friction factor, and found a very strong influence of the inner surface on the velocity distribution in the outer region of the annulus. We will deal with this in more detail later in the paper.

By the use of these graphs and empirical correlations, plus the conditions of continuity and of equal pressure in each cross section of the annulus, it is possible to transform the global data of the annulus to data referred to the inner rough region of the annulus only. The same procedure can be applied to use these data to predict friction and heat-transfer coefficients for clusters of rough rods contained in smooth shrouds [21].

3.3. The Maubach transformation and the shift of the position of no shear

The Hall and the Wilkie transformation methods are both assuming that in each cross section of the annulus the line of shear stress equal zero is coincident with the line of maximum velocity. Now, this is true with laminar flow and with turbulent velocity profiles symmetric in respect of the velocity maximum. These profiles occur with good approximation, for instance, with turbulent flow in annuli with relatively high radius ratios ($r_1/r_2 \geq 0.3$). But this is not true anymore for strongly asymmetric velocity profiles which occur in presence of an effective roughness at the inner surface of the annulus. Kjellström and Hedberg [22] explained theoretically and showed by experiment that indeed there was no coincidence between line of zero shear stress and line of maximum velocity in an annulus with a rough central rod, the position of no shear being shifted towards the outer smooth surface. In 1967 Wilkie *et al.* [23] carried out friction factor measurements in rectangular channels with walls of identical and non-identical roughnesses. These experiments proved experimentally the breakdown of the Hall transformation. Wilkie attributed this breakdown to the shift in the position of no shear in respect to the

position of maximum velocity and to the failure of the equivalent hydraulic diameter concept to correlate data from different shapes (in this context rectangular channel and annulus) exactly.

In 1971 Maubach and Rehme [24] published collected experimental data of various authors which proved again the non-coincidence of the two lines in annular and rectangular channels with smooth and rough surfaces. Recently Rehme [25] has shown that this non-coincidence or shift exists also in smooth annuli with very low radius ratios. In this case however the shift of the position of no shear is in the direction of the inner smooth surface of the annulus. He explains this shift by the fact that in presence of non-symmetric velocity profiles there is a transport of turbulent kinetic energy from the more energetic outer region into the less energetic inner region of the annulus. The same reasoning, of course, explains the shift of the position of no shear towards the outer smooth surface of the annulus in presence of an effective inner rough surface, because in this case the inner region of the annulus is the more energetic due to the enhanced friction at the rough inner surface.

In 1969 Maubach [26, 27] suggested for the annulus a transformation method which had already been implicitly used by Schlichting for rectangular channels [13]. Maubach assumes that the Nikuradse velocity profiles in tubes [equations (1) and (2)] are valid for the outer and inner regions respectively of an annulus with a central rough rod, and that the surface of no shear is given by the intersection of the two velocity profiles starting from the respective walls. Although mathematically at this intersection the velocity has a maximum, he shows that the agreement with the line $\tau = 0$ experimentally determined by Kjellström and Hedberg is excellent. At the intersection of the two velocity profiles one has:

$$\frac{u_{\max}}{(\tau_1/\rho_1)^{\frac{1}{2}}} = 2.5 \ln \left(\frac{r_0 - r_1}{h} \right) + R(h^+) \quad (19)$$

$$\frac{u_{\max}}{(\tau_2/\rho_2)^{\frac{1}{2}}} = 2.5 \ln \left[\frac{r_2 - r_0}{v_2} (\tau_2/\rho_2)^{\frac{1}{2}} \right] + 5.5. \quad (20)$$

Integrating equations (2) and (1) one obtains the friction factors for the inner and outer regions of the annulus:

$$\left(\frac{2}{f_1} \right)^{\frac{1}{2}} = 2.5 \ln \left(\frac{r_0 - r_1}{h} \right) + R(h^+) - G_1 \quad (21)$$

$$\left(\frac{2}{f_2} \right)^{\frac{1}{2}} = 2.5 \ln \left[\frac{r_2 - r_0}{v_2} (\tau_2/\rho_2)^{\frac{1}{2}} \right] + 5.5 - G_2 \quad (22)$$

where

$$G_1 = \frac{3.75 + 1.25r_0/r_1}{1 + r_0/r_1} \quad (23)$$

$$G_2 = \frac{3.75K_0 + 1.25r_0/r_2}{1 + r_0/r_2} \quad (24)$$

and $K_0 = 1.0576$ is an empirical factor which takes into account the viscous sublayer near the smooth surface in the integration. The conditions that at the intersection of the two velocity profiles the velocities

are equal [u_{\max} of equation (19) equals u_{\max} of equation (20)], that the pressure is constant in an annulus cross section, the equation of continuity and equations (21), (22) result in the following relationship:

$$\left(\frac{2}{f}\right)^\dagger = \frac{\beta^2 - \alpha^2}{1 - \alpha^2} \left(\frac{\beta^2 - \alpha^2}{\alpha(1 - \alpha)}\right)^\dagger \left\{ \frac{(1 - \beta^2)\alpha}{\beta^2 - \alpha^2} A - G_1 \right\} + \frac{1 - \beta^2}{1 - \alpha^2} \left(\frac{1 - \beta^2}{1 - \alpha}\right)^\dagger \{A - G_2\} \quad (25)$$

with

$$A = 2.5 \ln \left[\frac{1 - \beta}{2(1 - \alpha)} \left(\frac{1 - \beta^2}{1 - \alpha}\right)^\dagger Re \left(\frac{f}{2}\right)^\dagger \right] + 5.5 \quad (26)$$

and

$$\frac{r_1}{r_2} = \alpha, \quad \frac{r_0}{r_2} = \beta. \quad (27)$$

Once Re , f and α are known, equations (23)–(27) allow to calculate β (that is the position of the zero shear stress line) by numerical iteration. Re and f refer to the whole annulus and can be obtained by the measurements of mass flow and of pressure drop. Finally equations (19)–(22) allow the determination of f_1 , f_2 and $R(h^+)$.

The differences between the Maubach's and the Wilkie's methods are basically two. For Wilkie the friction characteristics of the inner rough surface are represented by the integral quantity f_1 , for Maubach they are, like for Nikuradse, by the parameter $R(h^+)$ supposedly independent of the shape of the channel delimiting the flow (macroscopic geometry). Secondly, for Maubach, the friction factor of the outer smooth surface, being derived from an integration of equation (1), is more or less equal to the friction factor of a smooth tube (in fact it is about 3–4% higher), while the Wilkie transformation method produces friction factors at the outer smooth surface which appear to be 1.5 times [20] and sometimes up to two times [28] higher than those of a smooth tube, a fact which is a bit difficult to understand. Because the total friction factor of the annulus must be the same, Wilkie predicts systematically smaller friction factors for the inner rough surface than Maubach does. Wilkie himself admits that the data transformed by his method may be too small, when he checks them with integral experiments on a bundle of rough rods contained in a smooth shroud [29].

3.4. The Dalle Donne–Meerwald transformation

This method is essentially an extension of Maubach's method, which is valid in isothermal conditions only, to the non-isothermal case with heat transfer [30]. Dalle Donne and Meerwald take into consideration the difference in physical properties of the gas in the two regions of the annulus by calculating them at two different mean temperatures, which they derive from the empirical graphs of Wilkie [20]. In reference [31] Meerwald shows that these empirical correlations give mean gas temperatures in fair agreement with those obtained from the temperature profile measurements of Nunner in circular channels with internal roughness

[17], at least in the range of Reynolds number from which they were obtained by Wilkie ($8 \times 10^4 \leq Re \leq 1.3 \times 10^6$). Equations (19)–(24) remain still valid, while equations (25) and (20) are replaced by:

$$\left(\frac{2}{f}\right)^\dagger = \frac{\beta^2 - \alpha^2}{1 - \alpha} \left(\frac{\beta^2 - \alpha^2}{\alpha(1 - \alpha)}\right)^\dagger \left(\frac{\rho_1}{\rho}\right)^\dagger \times \left\{ \left(\frac{\rho_1}{\rho_2}\right)^\dagger \left(\frac{1 - \beta^2}{\beta^2 - \alpha^2}\right)^\dagger A - G_1 \right\} + \frac{1 - \beta^2}{1 - \alpha^2} \left(\frac{1 - \beta^2}{1 - \alpha}\right)^\dagger \left(\frac{\rho_2}{\rho}\right)^\dagger \{A - G_2\} \quad (28)$$

with

$$A = 2.5 \ln \left[\frac{1 - \beta}{2(1 - \alpha)} \frac{v}{v_2} \left(\frac{\rho}{\rho_2}\right)^\dagger \left(\frac{1 - \beta^2}{1 - \alpha}\right)^\dagger Re \left(\frac{f}{2}\right)^\dagger \right] + 5.5. \quad (29)$$

And the gas physical properties are evaluated at the two average temperatures of the inner and outer region T_1 and T_2 obtained by the following equations derived by the Wilkie empirical graphs [20]. For $Re_1 = 2 \times 10^5$ the curves can be correlated by the following equations:

$$T_2' = \frac{T_B}{0.902 + 0.098(T_W/T_B)} \quad \text{for } T_W/T_B < 1.25 \quad (30)$$

$$T_2' = \frac{T_B}{0.8848 + 0.11173(T_W/T_B)} \quad \text{for } T_W/T_B \geq 1.25$$

$$T_1' = T_2' [1.06 - 0.235(T_W/T_B) + 0.175(T_W/T_B)^2] \quad \text{for } T_W/T_B < 1.4 \quad (31)$$

$$T_1' = T_2' [0.731 + 0.245(T_W/T_B)] \quad \text{for } T_W/T_B \geq 1.4$$

and for $Re_1 \neq 2 \times 10^5$:

$$T_2 = \frac{T_2'}{1.0484 - 0.009133 \log_{10} Re_1} \quad (32)$$

$$T_1 = T_1' (1.0958 - 0.018066 \log_{10} Re_1).$$

To characterize their heat-transfer data Dalle Donne and Meerwald used the Dipprey and Sabersky factor, supposed, like $R(h^+)$, invariant of the macroscopic geometry and defined for the annulus by:

$$G(h^+)^\dagger = R(h^+) + \frac{f_1 - 1}{2St_1} \cdot \frac{1}{(f_1/2)^\dagger}. \quad (33)$$

The temperature difference between rough surface and gas used to obtain St_1 was $T_W - T_1$, where T_W was measured and T_1 calculated from the empirical equations (31) and (32).

3.5. The Warburton–Pirie transformation

This transformation method was developed at the Central Electricity Generating Board, Berkeley Nuclear Laboratories in England by Warburton and Pirie [32] and it is a refinement of the method of Wilkie. Like

†For gases the Prandtl number is more or less constant and equal to 0.7. We deal in our treatment with heat transfer with gases only, therefore we can assume $G(h^+, Pr) \equiv G(h^+)$. With gas experimental data only, it would be impossible to investigate the effect of the Prandtl number on $G(h^+)$ due to very small variations of the Prandtl number of gases.

Maubach, Warburton and Pirie tried to take into account the shift of the position of no shear.

For the determination of the friction factor of the outer smooth annulus surface they assumed an empirical correction factor $K_3 = f_2/f_0(Re_2)$ similar to that of Wilkie and produced an empirical expression which correlates K_3 with data relative to the inner rough surface:

$$K_3 = 1.036 + 0.0057 \frac{f_1}{f_0(Re_1)} \quad (34)$$

That is:

$$\begin{aligned} f_2 &= K_3 [0.014 + 0.125 Re_2^{-0.32}] \\ &= [0.014 + 0.125 Re_2^{-0.32}] \\ &\times \left[1.036 + \frac{0.0057 f_1}{0.014 + 0.125 Re_1^{-0.32}} \right] \end{aligned} \quad (35)$$

where the expression $f_0 = 0.014 + 0.125 Re^{-0.32}$ is the Drew, Koo, McAdams explicit approximation [33] of the Prandtl-Nikuradse universal law of friction for smooth pipes:

$$\frac{1}{(f_0)^{1/2}} = 4 \log_{10} [Re(f_0)^{1/2}] - 0.4 \quad (36)$$

which can be obtained by integration of equation (1) in a pipe.

The factor K_3 , as given by equation (35), however, is much less dependent on the friction factor f_1 of the inner rough surface than in the case of the Wilkie correlation. In other words here it is implied that the velocity distribution in the outer region of the annulus is still influenced by the inner rough surface, but much less than in the Wilkie case. Figure 1 shows the factor $K_3 = f_2/f_0(Re_2)$ as a function of $f_1/f_0(Re_1)$. For $f_1/f_0 = 10$, K_3 is equal to 1.625 with Wilkie, and only to 1.093 with Warburton-Pirie. The Maubach line in Fig. 1 is practically horizontal and illustrates the fact that he assumes that the velocity profile in the outer annulus region is unaffected by the inner rough surface. The Warburton-Pirie line represents an improvement on the Maubach line. Indeed while the Maubach method is merely based on the experimental data of Kjellström and Hedberg for the determination of the position of the line of no shear stress, the equation (35)

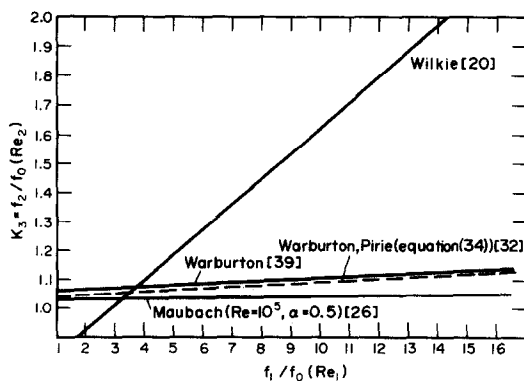


FIG. 1. Friction factor of the outer smooth channel of the annulus as a function of the friction factor of the inner rough rod for the various transformation methods.

of Warburton and Pirie is based on a much larger experimental evidence, for which care has been always taken to transform the data to the true line of zero shear [28, 34–38]. The differences among the Maubach, Warburton-Pirie and Warburton [39] lines in Fig. 1 are small in comparison with the Wilkie line, the Warburton line representing a small improvement on the Warburton-Pirie line based on a subsequent more accurate examination of even more experimental evidence. All three lines give values of K_3 between 1.03 and 1.06 when the abscissa is unity. This is realistic, as it has been experimentally verified that a smooth annulus will give a higher friction factor than a smooth pipe of the same equivalent diameter [40]. The Wilkie line gives the obviously wrong value $K_3 = 0.84$ for abscissa unity and has a considerably higher slope, apportioning too high a friction factor to the outer smooth channel. This is the result of the incorrect assumption regarding the position of the true surface of zero shear.

The second empirical factor K_1 , of the Warburton-Pirie transformation method equal to the ratio of absolute bulk temperature inside and outside the surface of zero shear, is taken from the Wilkie graphs and it is given by expressions similar to equations (30)–(32).

The third empirical factor K_2 , equal to the ratio of the mean velocities outside and inside the surface of zero shear, and which was taken by Wilkie as equal to 1.02 for a friction multiplier greater than five, is given by the expression

$$K_2 = 0.114 \frac{r_1}{r_2} + 0.97 \quad (37)$$

which correlates the experimental data within +8–5%, while in the Wilkie correlation the data scattered up to $\pm 11\%$.

Finally, Warburton and Pirie transformed the heat-transfer data using an empirical expression derived by Nathan and Pirie [41] and based on Pirie's results [38] using Hall's method:

$$\begin{aligned} \frac{St_1}{St} &= \left(\frac{f_1 D_h}{f D_{h1}} \right)^{0.5} (1.096 - 1.896 f_1) \\ &\times (1.255 - 0.0432 \log_{10} Re_1). \end{aligned} \quad (38)$$

Like in the Wilkie method, the conditions of continuity and equal pressure in the cross section of the annulus, plus the three empirical factors K_1 , K_2 , K_3 and the Stanton number transformation [equation (38)] allow to transform the global data of the annulus to data referred to the inner region of the annulus only. The method is thus conceptually the same as Wilkie's, but of course with more accurate correlations for the empirical factors and the Stanton number transformation.

In a recently published paper [42] Warburton and Pirie compare their method with Maubach's method of transformation of the friction factors. The friction factors transformed with Maubach lie about 4% above those transformed with Warburton-Pirie over the whole Reynolds number range investigated ($4 \times 10^4 \leq Re \leq 1.3 \times 10^6$).

3.6. The transformation of the present paper

The review of the transformation methods above indicates that none of these methods is completely satisfactory. On one side the Wilkie's and Warburton-Pirie's methods are based on merely empirical correction factors, on the other side the Maubach's and Dalle Donne-Meerwald's methods are based on the assumption that the surface of zero shear lies at the intersection of the logarithmic law velocity profiles applied at both walls of the annulus. Now the logarithmic law cannot hold exactly at the intersection of the two profiles, because this would imply a discontinuity of the first derivative of the velocity. The data of Nikuradse for tubes show quite clearly that the logarithmic law does not correlate exactly the velocities at the center of a pipe. Furthermore the high turbulence intensity caused by the rough inner surface should somewhat flatten the velocity profile in the smooth outer region. This would explain why the careful examination of the experimental data available performed by Warburton would suggest a slight increase of the friction factor of the outer smooth region as a function of the effectivity of the friction factor of the inner surface, while Maubach predicts practically no influence at all. The recent experimental investigations of Rehme for annuli with very low radius ratios [25], show that, while the velocity profile of the more energetic outer region follows quite well the Nikuradse law of the wall for smooth tubes [equation (1)], the velocity profiles of the less energetic inner smooth region tend to be flatter than the universal velocity profile, especially at lower Reynolds numbers. Rehme attributes this to the fact that the Reynolds numbers of the inner region are considerably smaller than those referred to the whole annulus, thus the flow regime in the inner region is not completely turbulent, but it is in a transition region between turbulent and laminar, and also to an effect of the flow in the outer region on the velocity profile of the inner region.

All this suggested to the authors a modification of the Maubach method which would take into account the Warburton experimental data and the observations of Rehme for smooth annuli with very small radius ratios, and at the same time maintain the use of the parameters $R(h^+)$ and h^+ , which have a less empirical nature than f_1 and $h/D_{h1}\dagger$ used by Wilkie and Warburton-Pirie, and therefore probably allow a better extrapolation of the data to different channel shapes, such as for instance to rod clusters. The velocity profile of the outer smooth region of the annulus is not assumed to follow the universal law of Nikuradse for smooth tubes [equation (1)] but the slope of the curve A_S is assumed to be a function of the friction factor of the inner rough rod:

$$u^+ = A_S \ln y^+ + 5.5. \quad (39)$$

Integration of (39) over y^+ for the outer annulus region

yields:

$$\bar{u}_2^+ = A_S \ln \left(\frac{r_2 - r_0}{v_2} u_2^* \right) + 5.5 - G_2 \quad (40)$$

where:

$$G_2 = \frac{3 + r_0/r_2}{2(1 + r_0/r_2)} A_S = \frac{3 + \beta}{2(1 + \beta)} A_S. \quad (41)$$

When one considers that $\bar{u}_2^+ = \bar{u}_2/u^* = (2/f_2)^\dagger$, $Re_2 = [2(r_2^2 - r_0^2)/r_2 v_2] \bar{u}_2$ and $\beta = r_0/r_2$, one can obtain the friction factor f_2 of the outer smooth region.

$$\left(\frac{2}{f_2} \right)^\dagger = A_S \ln \left[\frac{Re_2}{2(1 + \beta)} \left(\frac{f_2}{2} \right)^\dagger \right] + 5.5 - \frac{3 + \beta}{2(1 + \beta)} A_S \quad (42)$$

therefore:

$$A_S = \frac{(2/f_2)^\dagger - 5.5}{\ln \left[\frac{Re_2}{2(1 + \beta)} \left(\frac{f_2}{2} \right)^\dagger \right] - \frac{3 + \beta}{2(1 + \beta)}}. \quad (43)$$

The calculation of A_S is performed by iteration. In the first step of the iteration A_S is set equal to 2.5, then β, f_1, Re_1 etc. are calculated with the Maubach method [equations (25), (26)] for the isothermal case and with the equations (28), (29) for the case with heat transfer.

To obtain a new value of f_2 the Warburton empirical correlation [39] is used:

$$f_{2,n} = f_0(Re_{2,n-1}) [1.056 + 0.005(f_1/f_2)_{n-1}] \quad (44)$$

where $f_0(Re_{2,n-1})$ is derived from the Prandtl-Nikuradse universal law of friction for smooth pipes:

$$\frac{1}{(f_0)^\dagger} = 4 \log_{10} [Re_{2,n-1} (f_0)^\dagger] - 0.4 \quad (45)$$

and the suffix n indicates the n th iteration step. Then a new value of A_S is obtained from equation (43) and the calculation of β can be repeated, until β_n and β_{n-1} differ for less than a certain preset amount. Thus, the Warburton condition for the outer friction factor is taken into account and the velocity profile in the outer region becomes flatter (A_S less than 2.5). No Reynolds effect is considered in the Warburton empirical correction factor, and the flattening of the profiles due to the decrease of Reynolds number observed by Rehme cannot be allowed for by this method, but only the effect of the higher turbulent intensity of the inner rough region, which would correspond to the effect of the large difference in the area of the two surfaces of the annulus in the Rehme experiments with annuli with very low radius ratios.

Figure 2 shows a comparison of friction factors transformed with the methods illustrated in this paper. The experimental data on the figure have been obtained by J. T. Wilson of Winscale, England, by directly measuring the shear stress on the inner roughened surface by weighing [43]. The present method correlates the experimental data almost perfectly and considerably better than all the other transformation methods.

The second important difference of the present method regards the transformation of the heat-transfer data, that is the determination of the average gas tem-

$\dagger h/D_{h1}$ is the ratio of the roughness ribs height to hydraulic diameter of the inner region of the annulus.

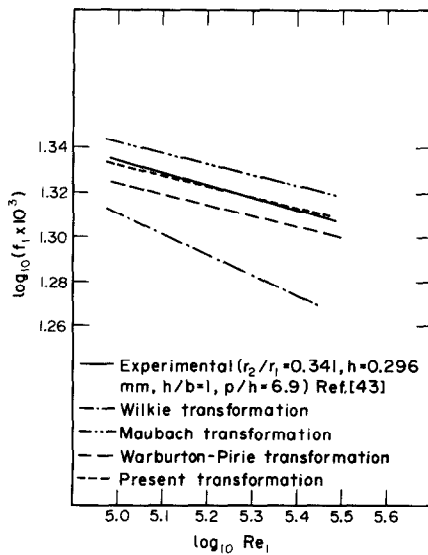


FIG. 2. Comparison of the experimental friction factors for a certain inner rough rod [43] with friction factors calculated with various transformation methods.

peratures inside and outside the line of zero shear and the definition of the parameter $G(h^+)$. At the start of the present experiment the experimental heat-transfer data were being transformed with the Dalle Donne–Meerwald's method illustrated in Section 3.4. This led to unexpected difficulties when we tried to transform the experimental data obtained at very low Reynolds numbers, where the inner rough surface of the annulus should "behave" like a smooth one. Although the values of $R(h^+)$ obtained were quite reasonable and presented a similar Reynolds number dependence as the Nikuradse sand-roughness values for tubes, the $G(h^+)$ values were much too low in comparison with those which Dipprey and Sabersky obtained for the flow in sand-rough tubes at low Reynolds numbers. This was obviously due to the choice of the average gas temperature T_1 for the calculation of the heat-transfer coefficient of the inner region. This temperature T_1 was obtained from equations (31), (32) derived by the Wilkie empirical graphs [20]. These, on the other side, hold for the range of Reynolds numbers 8×10^4 to 1.3×10^6 , and it is quite clear that the extrapolation of this empirical correlation down to Reynolds numbers of the order of a few thousand is not legitimate. This difficulty led the authors to a basically different approach for the transformation of the heat-transfer data.

With the Dalle Donne–Meerwald's transformation the parameter $G(h^+)$ is determined using the average gas temperature of the inner region of the annulus, the separation of the two regions being given by the position of no shear. In this, the transformation method is similar to all the previous ones, which are based on Hall's original assumption: to try to transform the data from a geometry (the annulus) in which the boundary conditions for the velocity profile ($\tau = 0$) and for the temperature profile ($q = 0$) are not coincident, to another geometry (central subchannels of a cluster

of rough rods) where these boundary conditions are coincident, it is necessary to build a hypothetical temperature profile for the inner region, which respects the condition of coincidence of $\tau = 0$ and $q = 0$. For the determination of this hypothetical temperature distribution according to Hall an integration constant is chosen so that "the new average gas temperature in the inner region is identical with the experimental value" [19]. That is, identical with the value T_1 obtained, for instance from the empirical graphs of Wilkie. Once T_1 is known, the actual shape of the hypothetical temperature profile does not affect at all the transformed values St_1 and $G(h^+)$. Seen in this light, the Hall's transformation, and all the others for that matter, is only a nice way to disguise the fact that the data are being transformed correctly for the friction, but, as far as heat transfer is concerned, they are simply referred to the average gas temperature of a region of the annulus which is not delimited by a well defined boundary condition such as $q = 0$. In an annulus the heat flux in radial direction is not vanishing at the surface of zero shear. At this surface the heat flux is considerably smaller than that at the inner heated rough surface, but it is not negligible. In experiments with annuli the condition $q = 0$ is generally given at the outer wall of the annulus due to the presence of the thermal insulation at the outside annulus wall. The average gas temperature T_1 of the inner region is higher than the mean gas bulk temperature T_b for the whole cross section of the annulus, and the transformed Stanton number St_1 is consequently higher than the Stanton number of the whole annulus (generally the difference is of the order of 5–10%).

In the light of these considerations let us consider the whole of the annulus cross section. We have seen that the Dipprey and Sabersky approach was successful in correlating the data of rough tubes. Let us assume, also for the annulus, that the temperature distribution in radial direction is given by:

$$t^+ = A_H \ln \frac{y}{h} + G(h^+), \quad (46)$$

valid in the whole cross section of the annulus, starting from the inner rough surface, across the line of zero shear, up to the outer wall of the annulus, which represents the adiabatic surface. In the following we shall try to determine the two still unknown parameters A_H and $G(h^+)$.

While the value of the slope of the velocity profile A_M is well established ($= 2.5$), the choice of a numerical value for the parameter A_H requires careful examination. Gowen and Smith found by experiment that for gases flowing in smooth tubes $A_H = 2.2$ [44], which is in agreement with the theoretical predictions of Landau and Lifshitz [45] and of Spalding [46]. Gowen and Smith found, also experimentally, for gases flowing in rough tubes the value $A_H = 2.7$ [47]. On the other hand the ratio A_H/A_M is equal, according to the above mentioned theoretical predictions, to the turbulent Prandtl number $Pr_t = \epsilon_M/\epsilon_H$, making possible a prediction of A_H knowing the values of A_M and of Pr_t .

Now, for gases the turbulent Prandtl number $Pr_t = \varepsilon_M/\varepsilon_H$ averaged in a pipe section is always slightly less than 1. Schlichting for instance suggests an average value of 0.86 [14] based on data of Ludwig [48] and Quarmby-Quirk an average value of 0.78 [49]. Thus a value for A_H greater than A_M seems to be too high. This consideration and the fact that the experimental determination of A_H by temperature traverses is always subjected to considerable uncertainty lead us to assume, like Dipprey and Sabersky, $A_H = 2.5$. In the present paper we shall confine ourselves to flow of gases and shall always assume $A_H = 2.5$.

This hypothesis simplifies considerably the calculations. Indeed it can be shown that, for flows in channels confined by rough heat-transfer surfaces only, in general one has:

$$G(h^+) = R(h^+) + \frac{\frac{f_R}{2St_R} - 1}{(f_R/2)^{\frac{1}{2}}} + \left(\frac{A_H}{A_M} - 1\right) \left[R(h^+) - \left(\frac{f_R}{2}\right)^{\frac{1}{2}} \right] \quad (47)$$

which can be obtained from equations (2) and (11) with A_M and A_H in place of 2.5 respectively and which reduces to the Dipprey-Sabersky equation for $A_H/A_M = 1$.

Contrary to the case of equations (16) and (47), which are valid for flows in channels confined by rough heat-transfer surfaces only, we determine the parameter $G(h^+)$ by measurements in annuli delimited by an inner rough heat-transfer surface and an outer adiabatic smooth surface. We have therefore to use other equations.

Considering the definition of t^+ (see Nomenclature) equation (46) becomes for an annulus:

$$T = T_W - \frac{q'_{g1}}{\rho_B c_{pB} u_1^*} \left[2.5 \ln \left(\frac{r-r_1}{h} \right) + G(h^+) \right] \quad (48)$$

where T_W is the temperature of the inner rough wall, q'_{g1} is the heat flux to the gas from the inner surface, $u_1^* = (\tau_1/\rho_1)^{\frac{1}{2}}$ is the friction velocity relative to the inner rough surface, ρ_B and c_{pB} are the relevant physical properties of the gas calculated at the mean gas bulk temperature T_B for the whole annulus. We neglect the heat flux to the gas from the outer surface q'_{g2} , which is always much smaller than q'_{g1} , as well as the difference between the friction velocities relative to the outer surface and to the inner surface respectively, in the outer region of the annulus. In the course of the evaluation of the present experiment we tried to calculate a radius r_m at which the two logarithmic temperature profiles starting from the two surfaces would intersect, as Dalle Donne-Meerwald did for the case of the smooth annulus [40], but this radius r_m was always very near to r_2 indicating that our assumption is quite legitimate.

At the outer wall of the annulus equation (48) becomes:

$$T_{Wa} = T_W - \frac{q'_{g1}}{\rho_B c_{pB} u_1^*} \left[2.5 \ln \left(\frac{r_2-r_1}{h} \right) + G(h^+) \right] \quad (49)$$

T_{Wa} , T_W , q'_{g1} are measured during the experiment. ρ_B , c_{pB} are known because we measure the gas pressure along the tube and determine the mean gas bulk temperature from the heat quantity given to the gas and the mass gas flow. u_1^* is known once β has been calculated with the method illustrated above [equations (39) to (45)]. And $G(h^+)$ can be obtained from the following equation derived from equation (49):

$$G(h^+) = \frac{(T_W - T_{Wa})\rho_B c_{pB} u_1^*}{q'_{g1}} - 2.5 \ln \left(\frac{r_2-r_1}{h} \right). \quad (50)$$

With the Dalle Donne-Meerwald transformation method the average gas temperatures T_1 and T_2 on each side of the line of zero shear used to determine β were given by the Wilkie empirical correlations. Here we shall suggest a new method to determine T_1 and T_2 . A method which is consistent with the assumption that the universal logarithmic temperature profile is valid over the whole of the annulus.

The mean gas bulk temperatures of the two regions of the annulus are:

$$T_1 = \frac{2}{c_{p1} u_1 \rho_1 (r_0^2 - r_1^2)} \int_{r_1}^{r_0} u \rho c_p T r dr \quad (51)$$

$$T_2 = \frac{2}{c_{p2} u_2 \rho_2 (r_2^2 - r_0^2)} \int_{r_0}^{r_2} u \rho c_p T r dr. \quad (52)$$

Equations (51), (52) cannot yield the values of T_1 and T_2 because for gases ρ is directly proportional to $1/T$. The product $u \rho c_p$ under the integral operator can be well approximated with its average value:

$$T_1 \approx \frac{2}{r_0^2 - r_1^2} \int_{r_1}^{r_0} T r dr \quad (53)$$

$$T_2 \approx \frac{2}{r_2^2 - r_0^2} \int_{r_0}^{r_2} T r dr. \quad (54)$$

Now, considering equation (48) we can perform the integration and obtain T_1 and T_2 :

$$T_1 = T_W - \frac{q'_{g1}}{\rho_B c_{pB} u_1^*} \left[2.5 \ln \left(\frac{(\beta-\alpha)r_2}{h} \right) - 2.5 \frac{1.5 + 0.5\beta/\alpha}{1 + \beta/\alpha} + G(h^+) \right] \quad (55)$$

$$T_2 = T_W - \frac{q'_{g1}}{\rho_B c_{pB} u_1^*} \times \left\{ \frac{2.5}{1 - \beta^2} \left[(1 - \alpha^2) \ln \left(\frac{(1-\alpha)r_2}{h} \right) - (\beta^2 - \alpha^2) \ln \left(\frac{(\beta-\alpha)r_2}{h} \right) - \frac{1 + 2\alpha - \beta^2 - 2\alpha\beta}{2} \right] + G(h^+) \right\}. \quad (56)$$

Applying the same approximated procedure to the whole of the annulus cross section, one would obtain the mean gas bulk temperature T_B :

$$T_B = T_W - \frac{q'_{g1}}{\rho_B c_{pB} u_1^*} \left[2.5 \ln \left(\frac{(1-\alpha)r_2}{h} \right) - 2.5 \frac{1.5 + 0.5(1/\alpha)}{1 + 1/\alpha} + G(h^+) \right]. \quad (57)$$

Equation (57) yields the approximated value of $G(h^+)$:

$$G(h^+)^* = \frac{(f/2)^{\frac{1}{2}} \left(\frac{\rho_B}{\rho_1}\right)^{\frac{1}{2}} \left(\frac{\beta^2 - \alpha^2}{\alpha(1-\alpha)}\right)^{\frac{1}{2}}}{St} - 2.5 \ln \left(\frac{(1-\alpha)r_2}{h} \right) + 2.5 \frac{1.5 + 0.5(1/\alpha)}{1 + 1/\alpha} \quad (58)$$

In [2] it is shown that the numerical values of $G(h^+)$ and $G(h^+)^*$ do not differ appreciably, indicating that the different approximations performed in obtaining both, and the values of T_1 and T_2 , are quite good.

The value of $G(h^+)$ from equation (50) is of course more exact than that of equation (58) because it is derived from two temperature measurements in the annulus cross section, at both annulus surfaces, rather than one. Furthermore equation (50) does not derive from an approximated integration like equation (58) does.

With this method we obtain the parameter $G(h^+)$ of a temperature profile with well defined boundary conditions ($q_1 = q'_{q1}, q_2 \approx 0$) which are the same as those of the central subchannels of clusters of rough rods. In Section 4.4 we will see that this improvement in the transformation method, and the one in the calculation of β illustrated above, lead to very good agreement between our transformed experimental data and data for flow in tubes.

4. THE PRESENT EXPERIMENT

4.1. Background

The results of the heat-transfer experiments in annuli with an inner rough rod performed in the past at the Heat Transfer Laboratory of the Institute of Neutron Physics and Reactor Engineering of the Karlsruhe Nuclear Center have been published [30, 31, 50, 51]. The transformation of these experimental data was performed with the Dalle Donne–Meerwald method (Section 3.4).

In [30] Dalle Donne and Meerwald published the results of their experimental investigations with 15 rods roughened with thread-type ribs of trapezoidal profile, and heated at surface temperatures up to 1200°C. The $R(h^+)$ values for the fully rough regime could be correlated in terms of the product pitch/height times pitch/width $p^2/(hb)$ of the ribs only. Within the scatter of the experimental points no h/\hat{y} (\hat{y} = distance from the rough wall to the line of zero shear stress) or temperature ratio effects could be observed. The transformed heat-transfer data were correlated by the expression:

$$G(h^+) = 5.8h^{+0.2} Pr^{0.44} (T_w/T_E)^{0.2} \quad (59)$$

very similar to the Dipprey–Sabersky relationship [equation (18)]. The new factor $(T_w/T_E)^{0.2}$ introduced by Dalle Donne and Meerwald took into account of large variations of the gas physical properties due to the large temperature differences present in the gas field. This factor is the same as that found by Dalle Donne and Meerwald for turbulent flow of gases in smooth annuli [40]. A theoretical explanation of this factor can be found in [52].

In [51] Dalle Donne and Meerwald published some preliminary experimental data showing that for roughness ribs with rectangular profile the value of $R(h^+)$ for a certain roughness is not completely independent of the size of the smooth channel where the rough rod is contained, thus a more accurate correlation of $R(h^+)$ values should contain a h/\hat{y} parameter, equal to the ratio of the roughness height to the distance between the rough wall and the surface of zero shear, or, in other words, to the length of the velocity profile. We shall try to explain the reason of this h/\hat{y} effect during the discussion of the friction data of the present experiment. The Dalle Donne–Meerwald data could be approximated for $h/\hat{y} > 0.07$ by the expression:

$$R(h^+) = R'(h^+) [(h/\hat{y})/0.07]^{0.3} \quad (60)$$

With the help of this correction factor they produced a general correlation for fully rough regime $R(h^+)$ values and rectangular ribs, which they obtained with the transformation method of Section 3.4 from friction data measured by various authors in annuli, pipes and rod clusters. For $1 < p/h < 8$ the data were correlated by:

$$\begin{aligned} \text{for } 2 \leq p^2/hb \leq 4 \quad R'(h^+) &= 10 \\ \text{for } 4 < p^2/hb \leq 75 \quad R'(h^+) &= 20.6(p^2/hb)^{-0.52} \\ \text{for } 75 < p^2/hb < 1000 \quad R'(h^+) &= 3.25(p^2/hb)^{-0.092} \end{aligned} \quad (61)$$

and for $p/h < 8, 0.086 \leq h/b \leq 12.5$ by:

$$R'(h^+) = 1.13(p/h)^{0.45} - (1 + 0.045p/h) \log_{10}(h/b) \quad (62)$$

The same extensive literature survey lead to the conclusion that the exponent of h/\hat{y} in equation (60) was a function of the roughness rib shape. Namely, it was equal to 0.5 for circular profile ribs (wire roughness) and practically negligible for triangular and trapezoidal ribs. All the heat transfer data with gases ($Pr \approx 0.7$) from the literature, independently of the rib shape, were correlated for $h^+ \geq 50$ by:

$$G(h^+) = K_1 Pr^{0.44} h^{+K_2} (T_w/T_E)^{0.2} \quad (63)$$

with

$$\begin{aligned} K_1 &= 2 + 0.46R(h^+) \\ \log_{10} K_2 &= -0.435 - 0.0336R(h^+) \end{aligned} \quad (64)$$

To similar conclusions came a literature survey mainly on roughnesses with rectangular rib profiles performed by Baumann and Rehme but restricted to friction data only [53–55]. The data surveyed by their investigation covered a considerably larger range of geometry parameters, especially for h/\hat{y} :

$$\begin{aligned} 0.35 \leq p/h &\leq 196 \\ 0.02 \leq h/b &\leq 15.1 \\ 0.08 \leq h/\hat{y} &\leq 0.997 \end{aligned} \quad (65)$$

Their h/\hat{y} effect was given by:

$$R(h^+) - R'(h^+) = 1.490(h/\hat{y}) - 1.972(h/\hat{y})^2 \quad (66)$$

which for $h/\hat{y} > 0.08$ gives a correction much smaller than that from equation (60), the scatter of the points being very large (see Fig. 5 of [55]).

One of the reasons for the present experiment was to solve the discrepancy between equation (60) and

Table 1. Test section dimensions

	r_2 (mm)
Outer smooth tube "40"	20.23
Outer smooth tube "50"	24.89
Outer smooth tube "70"	35.00
Outer smooth tube "85"	42.45

Test section number	r_1 (mm)	p (mm)	h (mm)	b (mm)	p/h	$\frac{p-b}{h}$	h/b	$R(\infty)_{0.1}$
1	16.76	1.80	0.288	0.30	6.25	5.21	0.96	2.58
2	16.69	19.30	0.314	0.30	61.5	60.5	1.05	7.42
3	16.58	2.00	0.493	0.30	4.06	3.45	1.64	2.43
4	16.69	2.00	0.411	0.50	4.86	3.65	0.82	4.04
5	16.53	3.00	0.519	0.30	5.77	5.20	1.73	1.80
6	16.29	3.20	0.784	0.30	4.08	3.70	2.61	1.80
7	16.41	3.20	0.787	0.80	4.07	3.05	0.98	4.15
8	16.26	4.80	0.785	0.30	6.11	5.73	2.62	1.38
9	16.21	12.80	0.796	0.30	16.2	15.7	2.64	2.56
10	16.20	24.00	0.809	0.30	29.7	29.3	2.70	4.00

(66). We performed therefore very accurate isothermal pressure drop measurements on ten rods with different rectangular rib roughnesses. Each rod was tested in four outer smooth tubes of different diameters. Table 1 shows the dimensions of the smooth tubes and of the rough rods. The second reason was, of course, to obtain reliable values of $R(h^+)$ in the fully rough flow region and also in the transition region between "fully rough" and "hydraulically smooth" flow regime.

The third reason was to obtain reliable heat transfer data and further information on the temperature difference effects on $G(h^+)$ and on $R(h^+)$. Therefore we performed heat-transfer tests for two of the test sections of Table 1: test section number 8, which gave the lowest $R(h^+)$ values in the isothermal tests (the highest pressure drop) and test section number 10, which gave typically high values of $R(h^+)$. Each of the heat transfer tests was performed with the two outer smooth tubes of 50 and 70 mm inner diameter.

In Section 4.2 below we will describe the experimental apparatus and the procedure used to obtain the global heat transfer and friction data for the whole of the annulus. In Section 4.3 we will present the isothermal experimental friction results, in Section 4.4 the experimental results with heat transfer.

4.2. Apparatus and procedure

The experimental apparatus used in the present experiment is the same as that used for the experiments with smooth annuli reported in [40] and [56]. A detailed description of the apparatus and of the procedure used to obtain the experimental data is given in those references. Here we will present only the main aspects of them.

A turboblower driven by an electrical motor delivers air successively through an orifice plate assembly to measure flow rate, an adiabatic entrance length, an annulus formed by a stainless steel heater rod supported concentrically in a tube, and finally to atmosphere.

Electrical supply for the test section is obtained from a fixed ratio transformer (40 V, 2000 A maximum), the primary winding of this transformer being supplied by a voltage regulator, the output voltage of which may be varied from 0 to 220 V. The voltage regulator is connected to the supply net through a voltage stabilizer. Thus there is the possibility of varying continuously the power supply from 0 to 80 kW and to keep constant within $\pm 0.5\%$ any value in this range.

The temperature of the internal tube heated surface is measured by means of 16 Platinel or CrNi/Ni thermocouples introduced in the center of the heater element and electrically insulated with twin bore alumina tubing and then inserted into the wall of the stainless steel tube where they are peened over (Platinel thermocouples) or welded (CrNi/Ni), the hot junction of the thermocouple being always on the surface of the inner tube wall. Four of the sixteen thermocouples are placed at the opposite side of the remaining to check for possible eccentricities in the annulus. The position of the thermocouples in respect of the roughness ribs is so chosen that possible local temperature differences on the rod surface are eliminated by averaging the thermocouple readings.

The outside tube of the annulus is insulated by a 50 mm thick calcium silicate slab contained between two layers of asbestos tape each about 7 mm thick. Twenty-two CrNi/Ni thermocouples are welded to the outer surface of this tube.

In eighteen sections each 100 mm apart for the outer smooth channels of 40, 50 and 70 mm dia, and in nine sections each 200 mm apart for the outer smooth channel of 85 mm dia are placed static pressure measuring devices. In each section there are four pressure taps spaced at 90° . Thus one has the average static pressure in the section independently from local dissymmetries. In practice the four measured values in any section differed very little.

The gas temperatures at the inlet and at the outlet

of the test section were measured respectively by means of two and five Cr/Ni shielded thermocouples, of which the four nearest to the test section outlet were extra shielded with perforated alumina tubing to reduce possible thermocouple reading errors caused by heat radiated from the hot inner rough rod. The gas temperature measurements were checked at every test by means of a comparison between the measured electrical power and the thermal power (heat to gas, plus heat losses through insulation).

The distribution of the power produced by Joule effect in the heater rod is known by measuring the voltage distribution along the tube. One leg of each thermocouple fixed on the inner tube is used as a voltage tapping.

The determination of the heat losses in radial direction through the thermal insulation placed around the outer tube of the annulus was performed by means of the so called "static calibration". The annulus is placed horizontally and the space between the inner rough rod and outer smooth tube kept under vacuum to reduce the effects of natural convection in the annulus section. The electrical current through the inner rod is adjusted to raise its temperature to a certain value. When steady temperature conditions are reached the temperature distributions along the inner and outer tubes and the electrical power are measured. The temperatures on the wall of the inner and outer tubes are constant in the central portion of the test section for a considerable length. Over this section all the heat produced in the inner tube is lost radially outwards by radiation from the inner tube to the outer one and by conduction through the tube insulation. This heat may be calculated from the electrical input to the section. By repeating this experiment at convenient temperature intervals it is possible to obtain an empirical relationship between the heat losses by conduction through the thermal insulation and the outer tube wall temperature.

The static calibration allowed also the measurement of the relative total emissivity ϵ_{12} between the two concentric tubes as a function of temperature. For the central portion of the test section where the temperatures T_w and T_{wa} are constant, one can assume with a good approximation that the heat is transmitted by radiation in radial direction only. Thus one can use the formula valid for infinitely long concentric tubes

$$q_r = \frac{\sigma S_1}{\frac{1}{\epsilon_1} + \frac{S_1}{S_2} \left(\frac{1}{\epsilon_2} - 1 \right)} (T_w^4 - T_{wa}^4) = \epsilon_{12} \sigma S_1 (T_w^4 - T_{wa}^4). \quad (67)$$

The emissivity coefficient depends on both temperatures T_w and T_{wa} but, in first approximation, $\epsilon_{12} \approx \epsilon_1$ because $S_1/S_2 < 1$ and we can assume that ϵ_{12} depends only on T_w . With the static calibration and the use of equation (67) it is possible to give ϵ_{12} as a function of T_w for any test section.

During the tests the temperatures of inner and outer tubes, the voltage distribution along the inner tube and the pressure distribution along the annulus were measured.

The bulk gas total temperature was calculated in the following way. The test section is divided into twenty equal parts along the length. For each part the heat produced in the inner tube by Joule effect (q_e) is calculated, knowing the electrical current and the voltage drop in that particular section. From the average value of T_{wa} of the section and the heat losses curve given by the static calibration one obtains the heat loss through the lagging (q_l). The difference between heat produced and heat lost gives the heat to the gas (q_g). Dividing this by the gas mass flow one obtains the increment in enthalpy of the gas in this section. The gas enthalpy at the inlet of the annulus is obtained from the gas temperature and pressure which are known. From the gas enthalpy and pressure distribution along the test section, one can calculate the total gas bulk temperature along the annulus. The gas physical properties are from [57]. To calculate the heat which goes by convection from the inner tube directly to the gas, it was necessary to subtract from q_g the heat which goes by radiation from the inner tube to the outer-tube and then by convection from the outer tube to the gas (q_{g2}). q_{g2} is given by the difference between q_r , which one can obtain knowing T_w , T_{wa} , ϵ_{12} (from the static calibration) and q_l . Thus:

$$q_{g1} = q_g - q_{g2} = q_g - (q_r - q_l) = q_e - q_l - q_r + q_l = q_e - q_r. \quad (68)$$

The friction coefficients were calculated from the equation:

$$f = -\frac{r_2 - r_1}{p\gamma Ma^2} \frac{\partial}{\partial x} [p(1 + \gamma Ma^2)] \quad (69)$$

which requires the measurement of gas mass flow, pressure, and total gas temperature T_T along the test section. This equation takes into account the pressure drop due to acceleration. Its derivation is shown in [56]. Using equation (69), it is not necessary to calculate directly the static gas bulk temperature T_B , although the fluid properties are evaluated at T_B , as they should, and not T_T . The calculations of heat-transfer and friction coefficients were performed in twenty sections 10 cm apart. All the values given in the paper are averages of the nine sections between 80 and 160 cm distant from the point where the heating starts. In this central portion of the test section the heat flux to the gas was always almost exactly constant and the effect of axial conduction of heat along the test section walls was negligible.

In respect of the experiments of [30, 50, 51] the experimental equipment and the procedure to evaluate the data have been improved in many ways, namely: the four orifice (diameters 15.8, 36.2, 38.2, 64.3 mm) plate assemblies to measure the flow rate have been anew calibrated against each other and against a reference orifice plate assembly.

In the calculation of air flow due account is taken of the moisture content of the air.

Due account is also taken of the dimensional changes in both tubes of the annulus with temperature during the calculations of the friction and heat-transfer coefficients. The number of sections, where calculations

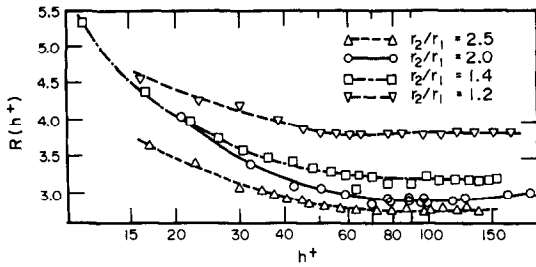


FIG. 3. Isothermal tests: $R(h^+)$ vs h^+ for the rough rod number 1.

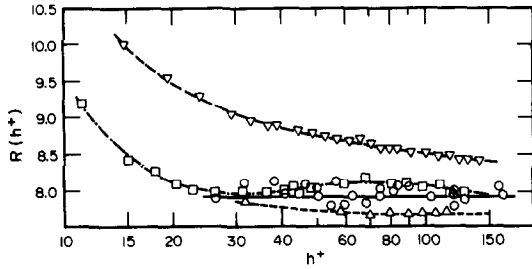


FIG. 4. Isothermal tests: $R(h^+)$ vs h^+ for the rough rod number 2.

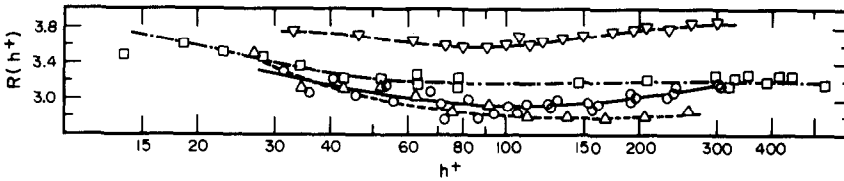


FIG. 5. Isothermal tests: $R(h^+)$ vs h^+ for the rough rod number 3.

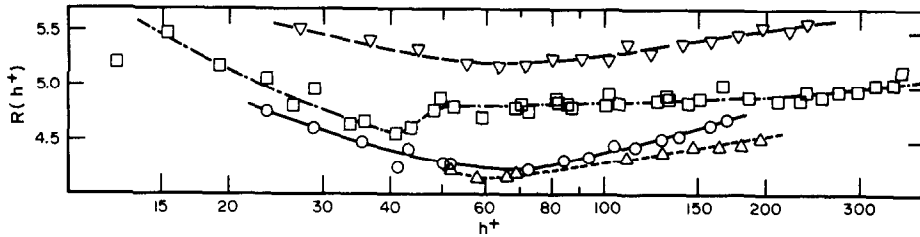


FIG. 6. Isothermal tests: $R(h^+)$ vs h^+ for the rough rod number 4.

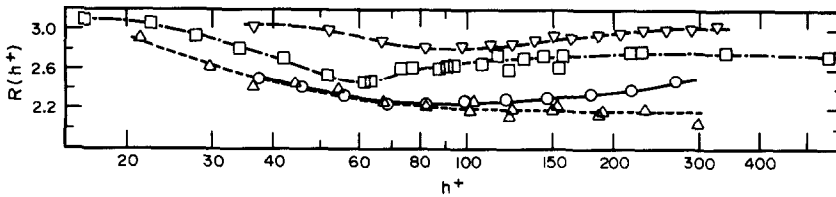


FIG. 7. Isothermal tests: $R(h^+)$ vs h^+ for the rough rod number 5.

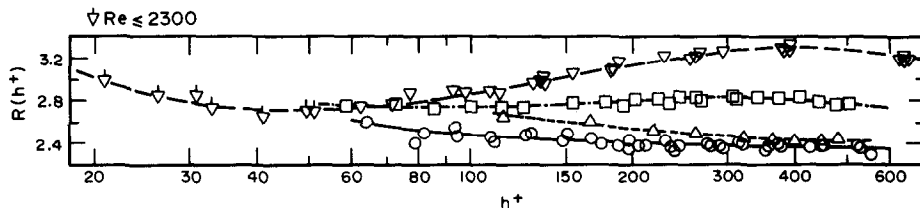


FIG. 8. Isothermal tests: $R(h^+)$ vs h^+ for the rough rod number 6.

have been performed, has been increased from 5 to 20.

More accurate instruments have been used for the measurement of the electrical voltage along the test section and, for the experiments with test sections 10/50, and 10/70, for the measurement of the gas pressure.

The number of pressure measurements along the test sections has been increased from 5 to 18 (channels 40, 50, 70) and to 9 (channel 85) respectively.

4.3. Isothermal experimental results

Figures 3–12 show the $R(h^+)$ values, plotted vs h^+ , of the ten different rods tested during the present experiment. These values have been obtained by means of friction factor measurements and the transformation method presented in this paper in Section 3.6. Each of the ten rough rods was tested in four outer smooth channels of different inner diameters (40, 50, 70, 85 mm), which correspond to annulus ratios of about 2.5, 2.0, 1.4 and 1.2 respectively.

In [2] detailed information is given on the experimental untransformed and transformed data both for the isothermal and thermal tests. Some of the points plotted in Fig. 3–12 are averages between two experimental results at the same gas flow, which were slightly

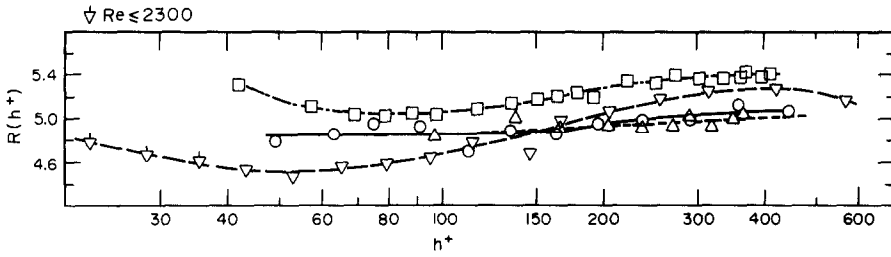


FIG. 9. Isothermal tests: $R(h^+)$ vs h^+ for the rough rod number 7.

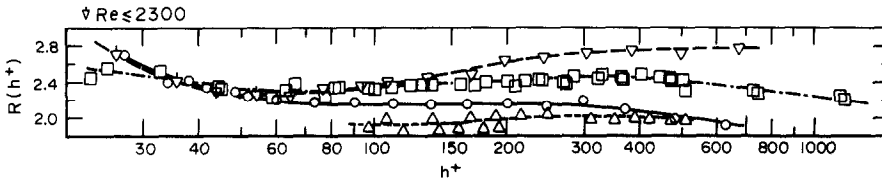


FIG. 10. Isothermal tests: $R(h^+)$ vs h^+ for the rough rod number 8.

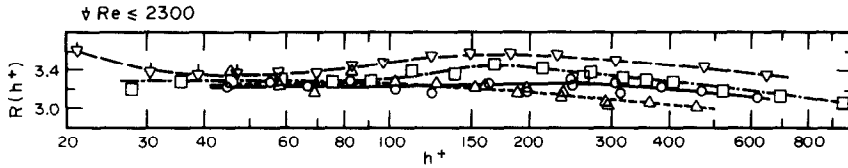


FIG. 11. Isothermal tests: $R(h^+)$ vs h^+ for the rough rod number 9.

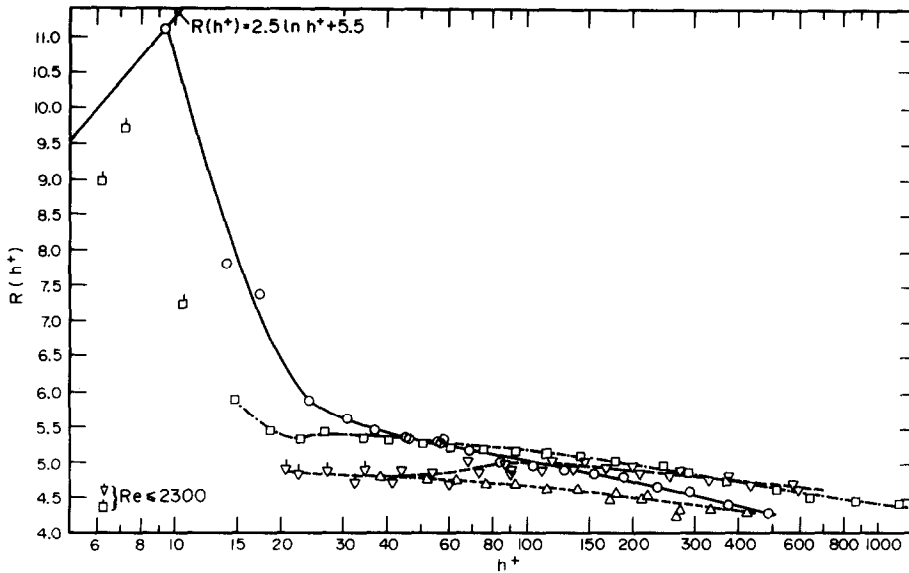


FIG. 12. Isothermal tests: $R(h^+)$ vs h^+ for the rough rod number 10.

different due to the use of two different instruments used to measure the pressure drops along the test sections. The two instruments were a "Betz" manometer and a variable slope manometer, which for low pressure drop measurements gave slightly different readings. For the test sections 10/50 and 10/70, both during the isothermal and the heat-transfer tests, we used therefore a series of membrane manometers (Baratron) with electronic digital readings, which allowed a considerably higher precision in the pressure drop measurement down to very low gas flows, and excellent

measurements of friction factors down to laminar flow regimes, as we will illustrate in the next section.

The scatter of the points of Figs. 3-12 look much higher than the directly measured experimental data would indicate. For instance a variation in $R(h^+)$ of 0.1 for test section 1/70 would correspond to a change in the transformed value f_1 of 1.6% only and in the directly measured friction factor for the whole annulus of 0.95% only.

Figures 3-12 show that the $R(h^+)$ values tend to increase, when the diameter of the outer channel

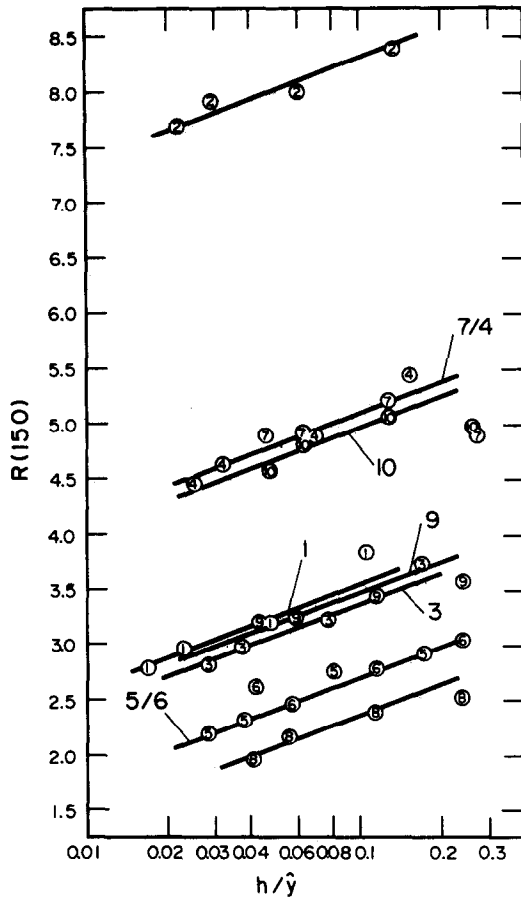


FIG. 13. $R(h^+) \text{ vs } h/\hat{y}$ for $h^+ = 150$.

decreases, that is when the ratio between the roughness height h and the length of the velocity profile (distance between the rough surface and the surface of zero shear) \hat{y} increases. This fact is illustrated even better by the Fig. 13 which shows the values of $R(h^+)$ at $h^+ = 150$ for the ten tested rough rods vs h/\hat{y} in a semilogarithmic graph. The scatter of the points is one order of magnitude less than that obtained in the literature survey of Baumann and Rehme (see Fig. 5 of [55]). This great improvement is probably due to the fact that in our case all the tests were performed at the same laboratory, and with great care, and the tests in various outer smooth channels were performed with exactly the same rough rods, thus eliminating possible effects due to not exact dimensions of the rods or of the roughness ribs, to rounding of the rib edges etc. Figure 13 shows quite clearly that the h/\hat{y} effect on $R(h^+)$ is additive and not multiplicative as was wrongly assumed in [51–53], i.e. it is the same whatever the absolute value of $R(h^+)$ is, for a certain constant value of h/\hat{y} . The data for $h^+ = 150$ can be correlated for $0.015 < h/\hat{y} \leq 0.235$ by the expression:

$$R(h^+ = 150) = R(h^+ = 150, h/\hat{y} = 0.01) + 0.4 \ln \left(\frac{h/\hat{y}}{0.01} \right) \tag{70}$$

With the Maubach transformation the h/\hat{y} effect would have been about 25% higher (see [2]).

Equation (70) agrees in the range up to $h/\hat{y} = 0.0235$

reasonably well with equation (60) obtained by Dalle Donne and Meerwald [51], however, Fig. 13 shows that an extrapolation of equation (60) to h/\hat{y} values of the order of 0.5 is not legitimate. Indeed for $h/\hat{y} > 0.235$ the $R(h^+)$ values decrease very rapidly as has been also noticed by Baumann and Rehme [55]. Equation (66) from [55] is more correct in its form than equation (60), but it underestimates the h/\hat{y} effect in the range investigated in the present experiment (which is the interesting one for the practical purpose of increasing the thermal performance of the roughness) almost by an order of magnitude.

In our opinion the h/\hat{y} effect in the range ≤ 0.235 can be explained as follows. We have already mentioned that the universal velocity distribution of Nikuradse, equation (2), cannot be valid in the region of zero shear for reasons of continuity in the velocity profile. Nikuradse, and many other experimenters after him, observed that in this region the velocity profile is higher than the profile given by equation (2). It can be seen from the experiments that the size of this region of discrepancy is always more or less the same, therefore its percentage effect is greater by shorter lengths of the velocity profiles, that is for higher values of h/\hat{y} . Now, when we measure the friction factor, we actually measure the average value of the dimensionless velocity profile $[\bar{u}^+ = (2/f)^{1/2}]$ and by assuming that equation (2) is valid, we obtain $R(h^+)$. For instance for a tube:

$$R(h^+) = \bar{u}^+ - 2.5 \ln(R/h) + 3.75. \tag{71}$$

What we measure, however, is \bar{u}^+ of the actual velocity profile and not the average value of a perfectly logarithmic profile. Therefore we obtain a higher value of $R(h^+)$, and this increase is more pronounced when the region of discrepancy from the logarithmic profile is larger relatively to the length of the velocity profile, i.e. for greater values of h/\hat{y} . The h/\hat{y} effect cannot, at least for this type of roughness ribs, be explained by the choice of the definition of the hydraulic diameter (volumetric, based on the tip or the root of the ribs) as postulated in [55]. Indeed it can be seen from the Fig. 13 that the h/\hat{y} effect is the same for the rod 2 as for the others. Now with test Section 2, which has $p/h = 61.5$, there is practically no “shift of the true origin of the averaged velocity profile in the direction of the flow” [55] if the height of the rib increases, but the h/\hat{y} effect is exactly the same as for roughnesses with $p/h = 4$. The h/\hat{y} effect is always the same whatever are the geometrical parameters of the rectangular ribs, therefore its explanation should be sought far from the ribs (region of zero shear) and not near the ribs.

The explanation of the h/\hat{y} given above is in contradiction with the findings of the literature survey of Dalle Donne and Meerwald [51] which showed that the h/\hat{y} effect is a function of the rib shape (circular, triangular, etc.). However, we have already seen that correlations of experimental data coming from a literature survey of many different sources can be in considerable error when relatively moderate differential effects, like h/\hat{y} 's, are investigated. To really have the

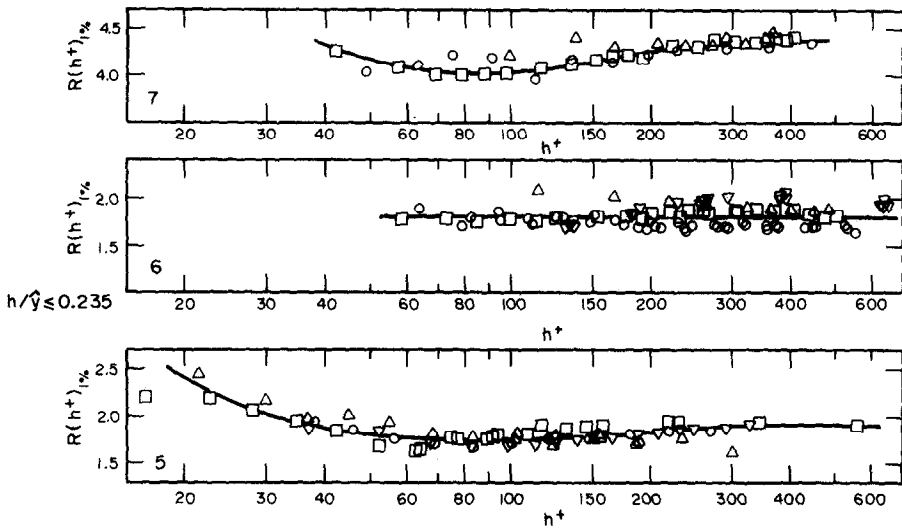


FIG. 14. $R(h^+)$ vs h^+ for $h/\hat{y} = 0.01$ and rough rod numbers 5, 6 and 7.

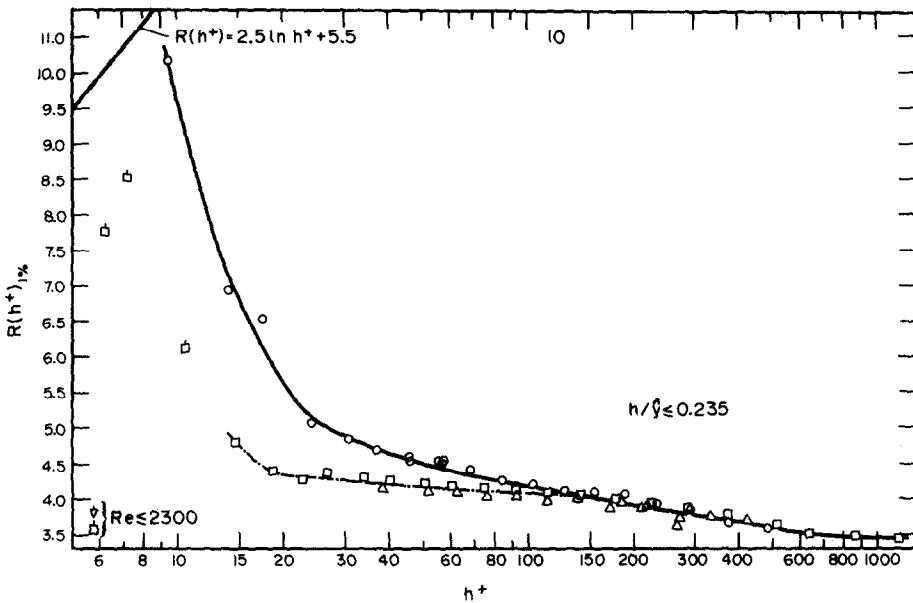


FIG. 15. $R(h^+)$ vs h^+ for $h/\hat{y} = 0.01$ and for rough rod number 10.

h/\hat{y} effect for triangular or circular ribs, it should be necessary to make the same sort of experiment which we made for rectangular ribs and which we report in this paper.

Figure 13 shows for $h/\hat{y} > 0.235$ a rapid decrease of $R(h^+)$. In this range the height of the ribs is too large in comparison with the length of the velocity profile and it has no meaning any more to speak of artificial roughness or of logarithmic velocity profile, average of cross sections where there is the rib and cross sections where there is no rib, due to the considerable contraction of the flow vein over the ribs. Indeed we calculated for instance the friction factor of the test section 7/40 ($h/\hat{y} = 0.26$) considering it as an orifice plate and we obtained a very good agreement with the measured experimental data.

Figures 14 and 15 show the parameter:

$$R(h^+)_{1\%} = R(h^+) - 0.4 \ln \left(\frac{h}{\hat{y}} / 0.01 \right) \quad (72)$$

vs h^+ for the test rods 5, 6, 7 and 10 investigated in the present experiment. They show that for $h^+ \geq 100$ (fully rough flow regime) the h/\hat{y} effect is more or less independent of h^+ . In this region of h^+ the universal velocity of Nikuradse [equation (2)] can be therefore written as:

$$\begin{aligned} u^+ &= 2.5 \ln \frac{y}{h} + R(h^+)_{01} + 0.4 \ln \left(\frac{h}{\hat{y}} / 0.01 \right) \\ &= 2.5 \ln \left(\frac{y}{h^{0.84} \hat{y}^{0.16}} \right) + R(h^+)_{01} + 1.84 \quad (73) \end{aligned}$$

where $R(h^+)_{1\%} = R(h^+)_{01}$ = value of $R(h^+)$ for $h/\hat{y} = 0.01$.

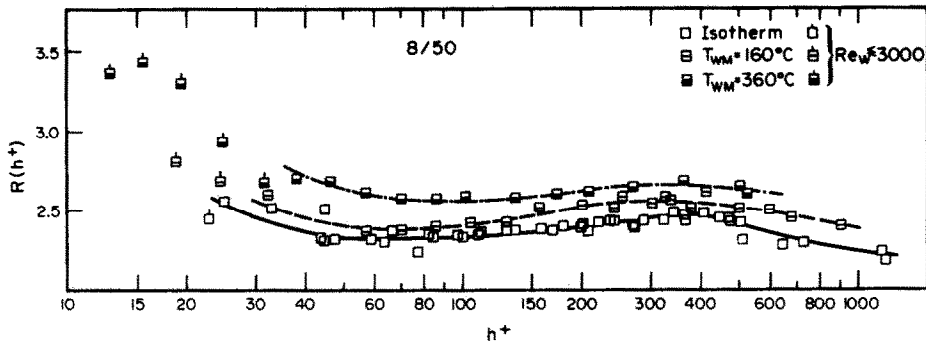


FIG. 16. Thermal tests: $R(h^+)$ vs h^+ for test section 8/50.

Equation (73) could have been also written as:

$$u^+ = 2.5 \ln \left(\frac{y}{h^{0.84} \delta^{0.16}} \right) + R(h^+)_{h/\delta=1} \quad (74)$$

but we prefer the form of (74) because $R(h^+)_{h/\delta=1}$ has no physical meaning.

4.4. Experimental results with heat transfer

Figures 16–19 show the $R(h^+)$ values plotted vs h^+ of the four test sections 8/50, 8/70, 10/50, 10/70, where 8 for instance denotes the number of the inner rough rod and 50 the diameter of the outer smooth channel. For each of the test sections three series of runs were carried out with maximum wall temperatures on the rough rod surface of $T_{WM} = 160, 360,$ and $500\text{--}600^\circ\text{C}$ respectively. Figures 20–23 show the same friction values, but this time plotted vs h_{eff}^+ . In both cases it is evident that the velocity profile [values of $R(h^+)$] is affected by the temperature level. This fact was not so evident in the experimental results of Dalle Donne and Meerwald [30, 50, 51] probably due to the larger scatter of their experimental points, due to the considerably less accuracy of their experiments.

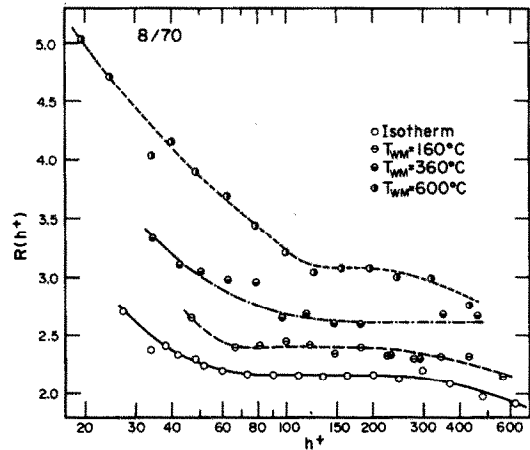


FIG. 17. Thermal tests: $R(h^+)$ vs h^+ for test section 8/70.

Figure 19 shows also the $R(h^+)$ values obtained by Webb for flow inside tubes with rectangular ribs with $p/h = 20$ and 40 respectively [58]. For the rod “10”, $p/h = 29.7$, while the values of h/b and h/δ for 10/70 are slightly different from those of Webb ($h/b = 1.94$,

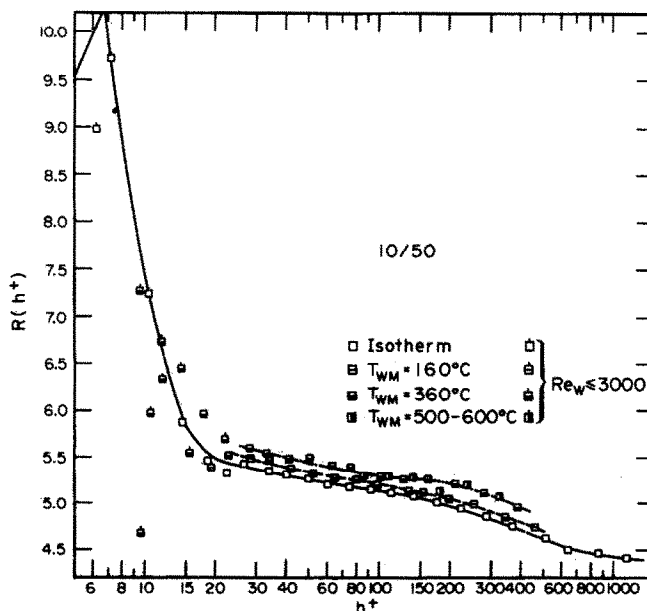


FIG. 18. Thermal tests: $R(h^+)$ vs h^+ for test section 10/50.

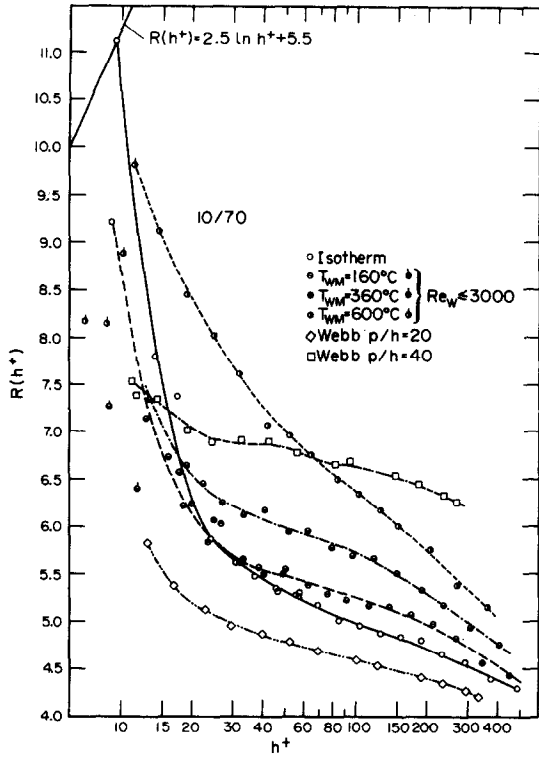


FIG. 19. Thermal tests: $R(h^+)$ vs h^+ for test section 10/70.

$h/\hat{y} = 0.04$ for Webb's ribs, $h/b = 2.70$, $h/\hat{y} = 0.064$ for test section 10/70). The h/b and h/\hat{y} effects on $R(h^+)$ when evaluated with [51] and equation (70) respectively are about the same in absolute value but of different sign and cancel each other. Figure 19 shows that the isothermal $R(h^+)$ values for test section 10/70 lie between those of Webb as they should. The $R(h^+)$ values of 10/70 calculated with the Maubach transformation method would have been lower than those calculated with the present method. The data of Webb, being for flow through completely rough tubes, are of course not transformed and this better agreement of the $R(h^+)$ values shows again the improvement of the present transformation in respect of Maubach's one.

The Figs. 19 and 23 show that the $R(h^+)$ values increase considerably with decreasing h^+ , for h^+ smaller than 30 (transition region between "fully rough flow" and "hydraulically smooth flow" regime), the transition region being affected quite considerably both by the temperature level and the h/\hat{y} parameter. If the Reynolds number is sufficiently high ($Re_w > 3000$) the points reach the line of the hydraulically smooth flow regime:

$$R(h^+) = 2.5 \ln h^+ + 5.5 \quad (75)$$

obtained from equation (4) derived by Nikuradse, valid for small h^+ values.

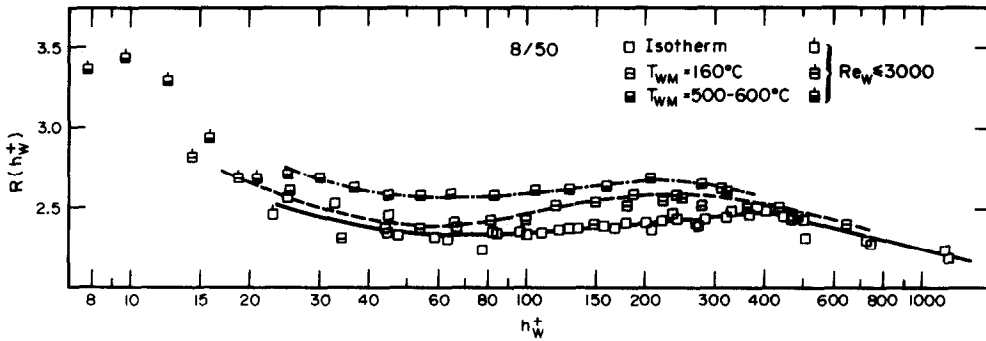


FIG. 20. Thermal tests: $R(h_w^+)$ vs h_w^+ for test section 8/50.

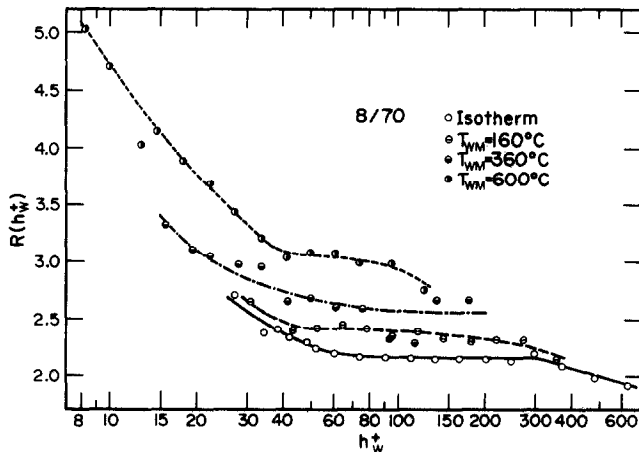


FIG. 21. Thermal tests: $R(h_w^+)$ vs h_w^+ for test section 8/70.

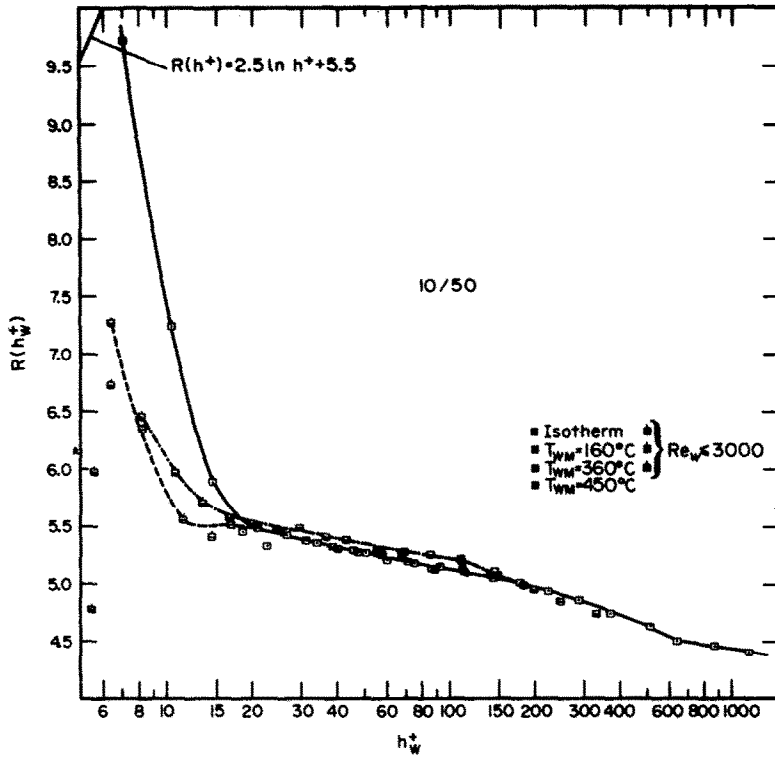


FIG. 22. Thermal tests: $R(h_w^+)$ vs h_w^+ for test section 10/50.

For $Re_w \leq 3000$ the $R(h^+)$ values decrease rapidly independently of the value of h^+ . These points lie obviously either in a region of transition between turbulent and laminar flow or they lie in the laminar region. These points have been plotted for completeness, but they have not really a physical meaning because the logarithmic velocity profile with a constant slope equal to 2.5, which defines $R(h^+)$, does not hold

in laminar flow, or in transitional flow between turbulent and laminar. The criterion $Re_w \leq 3000$, where Re_w is the Reynolds number for the whole of the annulus evaluated at the temperature T_w of the inner hot rough surface, has been suggested by the experiments of Dalle Donne and Bowditch for flow of gases inside tubes at high temperatures [59].

From Figs. 18, 19, 22 and 23 (and also from the Fig. 31) it appears that it is the Reynolds number h_w^+ based on the roughness rib height and on the gas properties evaluated at the temperature T_w of the inner hot rough surface, rather than h^+ , which establishes if the flow is in the fully rough region, in the turbulent smooth flow region [$R(h^+) = 2.5 \ln h^+ + 5.5$] or in the transition region in-between.

Figure 24 shows the product of the untransformed values $f \times Re$ vs T_w/T_B for the experiments where the flow was clearly laminar, the criterion of laminarity being that obtained by Dalle Donne and Bowditch for flow of gases inside tubes at high temperatures, that is $Re_w \leq 1800$ [59]. For $T_w/T_B = 1$ (isothermal tests) the product $f \times Re$ agrees very well with the theoretical value 24 calculated by Tiedt for concentric smooth annuli [60]. For $T_w/T_B \geq 1$ the experimental data of Fig. 24 can be correlated by:

$$f = \frac{24}{Re} \left(\frac{T_w}{T_B} \right)^{1.84} \quad (76)$$

The temperature effect is thus in good agreement with that found by Dalle Donne and Bowditch for laminar flow of gases inside tubes at high temperatures,

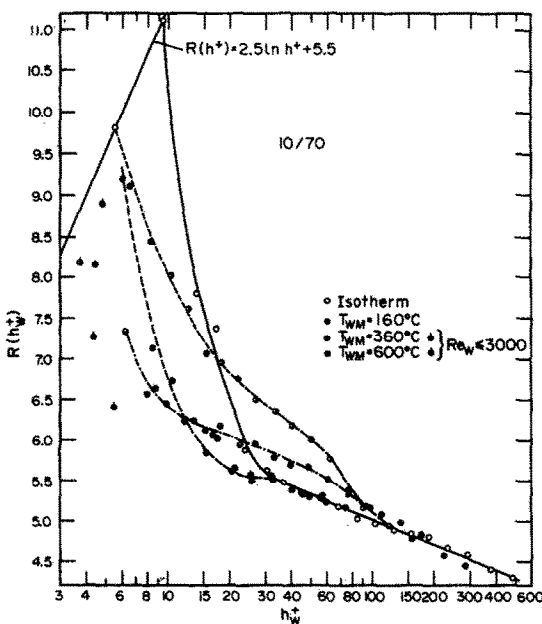


FIG. 23. Thermal tests: $R(h_w^+)$ vs h_w^+ for test section 10/70.

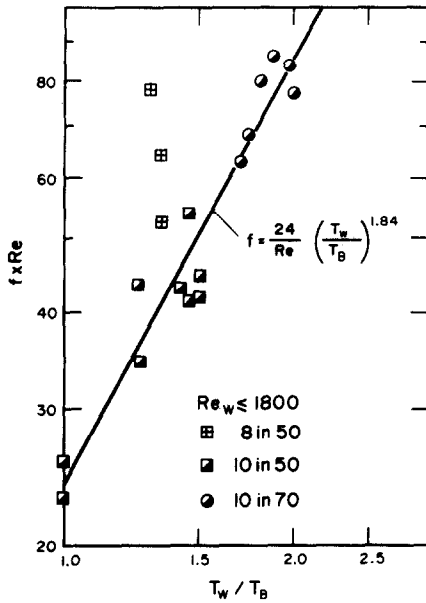


FIG. 24. The product $f \times Re$ vs T_w/T_B for the test runs in laminar flow.

i.e. $(T_w/T_B)^{1.68}$ [59]. Figure 24 shows how good were our pressure drop measurements with the Baratron manometers, even at very low flows (test sections 10/50 and 10/70). Indeed the data for the test section 8/50, obtained as an average between the readings of the Betz and the variable slope manometers, do not correlate as well as the previous.†

Figure 25 shows the values of $G(h^+)/Pr^{0.44}$ for the test section 10/70 plotted vs h^+ and Figs. 26–29 the same values vs h_w^+ for the four test sections investigated. The Prandtl number effect on the heat transfer parameter $G(h^+)$ was not investigated in the present experiment, because we made experiments with air only, i.e. at a Prandtl number practically constant. Therefore we assume a $Pr^{0.44}$ effect like Dipprey and Sabersky. Also here, like for $R(h^+)$, a temperature level effect is evident from the graphs. However, the lines at different temperature levels are parallel in the graphs with abscissa h_w^+ and they are not always parallel in the graphs with abscissa h^+ , (see also [2]), thus indicating that a correlation of the temperature effects is simpler with $G(h_w^+)$ function of h_w^+ than with $G(h^+)$ function of h^+ .

Figure 25 shows again the data of Webb for flow inside rough tubes for $p/h = 20$ and $p/h = 40$ [58].

†Subsequently K. Rehme has pointed out to the authors the fact that, if the laminar friction data of test section 8/50 would have been evaluated with a hydraulic diameter based on the tip of the roughness ribs, which is reasonable for a roughness with a relatively low value of $(p-b)/h$, also these friction data would have agreed much better with equation (76), the scatter of the points remaining higher than that for the friction data of the rod "10". On the other hand it is not reasonable to use the tip hydraulic diameter for the rod 10 because with a large value of $(p-b)/h$ [in this case $(p-b)/h = 29.3$] the flow reattaches again to the wall and thus occupies the main portion of the channel section. Here the volumetric hydraulic diameter is obviously a better geometrical parameter.

Webb's data agree very well with our data at low temperatures. Also Webb's data were obtained at low temperatures. This is, again, a confirmation of the present transformation method for heat transfer results. Indeed, if one would have used the T_1 value calculated with the Wilkie empirical graphs for the transformation of the heat transfer data, our values of the ratio $G(h^+)/Pr^{0.44}$ at low temperature and for the smallest values of h^+ would have lain up to 50% below Webb's data.

In [2] various methods are discussed to try to correlate the temperature effects both on the values of $R(h^+)$ and of $G(h^+)$, here we will report only the main results of these attempts. Figures 30 and 31 show the values of $R(h^+)_1$, that is the values corrected for the temperature effect (reduced to the temperature ratio equal one), for the test sections 8/50 and 8/70. Two correction factors have been tried. The first is for the correlation $R(h^+) vs h^+$:

$$R(h^+) - 0.8 \left(\frac{T_w}{T_1} - 1 \right)^{1.3} \quad (77)$$

and the second relative to the correlation $R(h_w^+) vs h_w^+$:

$$R(h_w^+) - \frac{5}{(h_w^+)^{\dagger}} \left(\frac{T_w}{T_1} - 1 \right)^2 \quad (78)$$

Figures 32 and 33 show the values of $R(h^+)_1$ for the test sections 10/50 and 10/70 corrected with this second method.

It is evident from the figures that this second parameter correlates the data better than the first, especially because, as we have already said, it is h_w^+ rather than h^+ , which decides if the $R(h^+)$ points are in the fully rough flow region [small variations of $R(h^+)$, high values of h_w^+], in the turbulent hydraulically smooth region [for $Re_w > 3000$ and low values of h_w^+ the points fall on the line $R(h^+) = 2.5 \ln h^+ + 5.5$], or in the transition region in between the two previous, while the value of Re_w decides if the flow is laminar ($Re_w \leq 1800$ whatever is the value of h_w^+), in the transition region between turbulent and laminar ($1800 \leq Re_w \leq 3000$) or turbulent ($Re_w > 3000$, whatever the value of h_w^+). For these flow regions (laminar and transitional between turbulent and laminar) the $R(h^+)$ values are considerably lower than the values for $Re_w > 3000$. As we explained already, the $R(h^+)$ points have no real physical meaning for $Re_w \leq 3000$.

Neither of the correlations chosen is able to correct for the temperature effect in the transition region between fully rough and hydraulically smooth flow. During the evaluation of the friction data of the present experiment we tried to use the Reynolds number $h_{h/2}^+$ based on the rib height h and on gas properties evaluated at a temperature $T_{h/2}$ given by the arithmetic average between the temperature of the rough surface T_w and the temperature at $y = h$, i.e.:

$$T_{h/2} = T_w - \frac{1}{2} \frac{q_{\theta 1}}{\rho_B c_{pB} u_{\theta 1}^{\dagger}} G(h^+) \quad (79)$$

The correlation $R(h_{h/2}^+) vs h_{h/2}^+$ was no better than the correlation in terms of $R(h_w^+) vs h_w^+$, therefore we abandoned it, due to its additional complication.

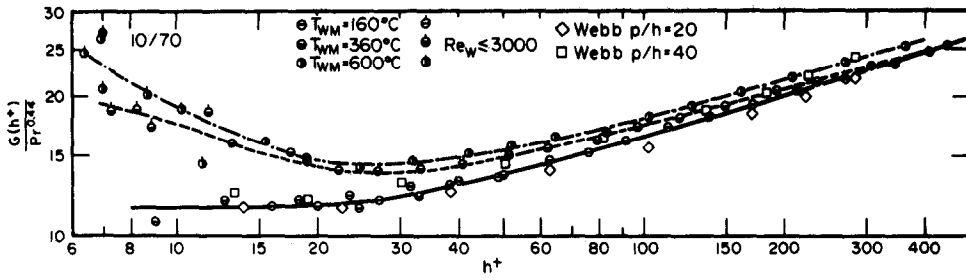


FIG. 25. Thermal tests: $G(h^+)/Pr^{0.44}$ vs h^+ for test section 10/70.

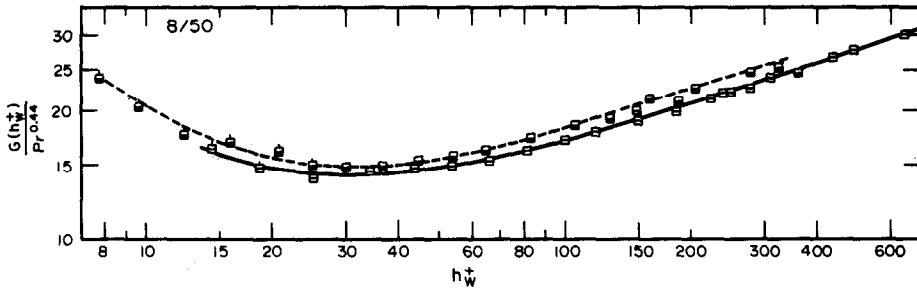


FIG. 26. Thermal tests: $G(h_w^+)/Pr^{0.44}$ vs h_w^+ for test section 8/50. (Symbols of Fig. 20.)

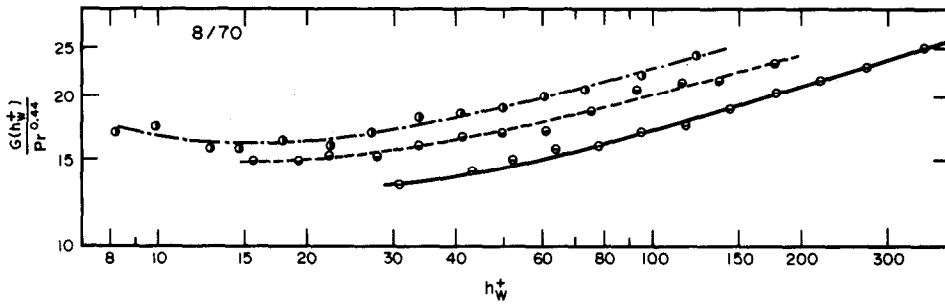


FIG. 27. Thermal tests: $G(h_w^+)/Pr^{0.44}$ vs h_w^+ for test section 8/70. (Symbols of Fig. 21.)

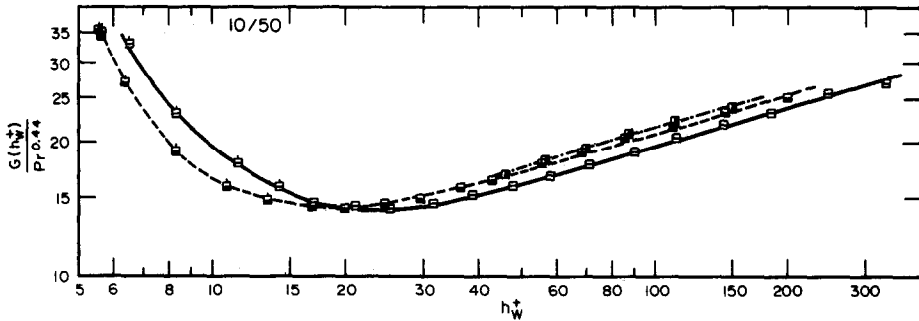


FIG. 28. Thermal tests: $G(h_w^+)/Pr^{0.44}$ vs h_w^+ for test section 10/50. (Symbols of Fig. 22.)

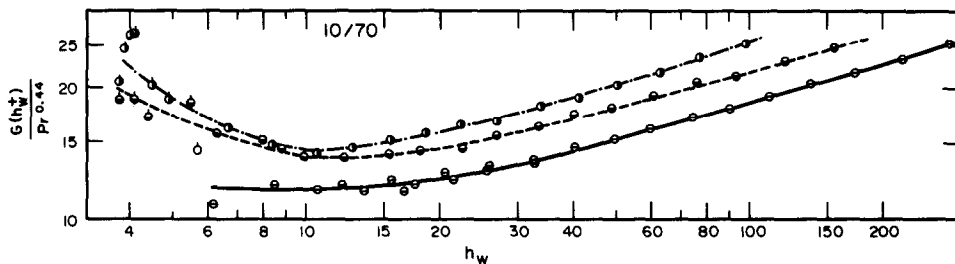


FIG. 29. Thermal tests: $G(h_w^+)/Pr^{0.44}$ vs h_w for test section 10/70. (Symbols of Fig. 23.)

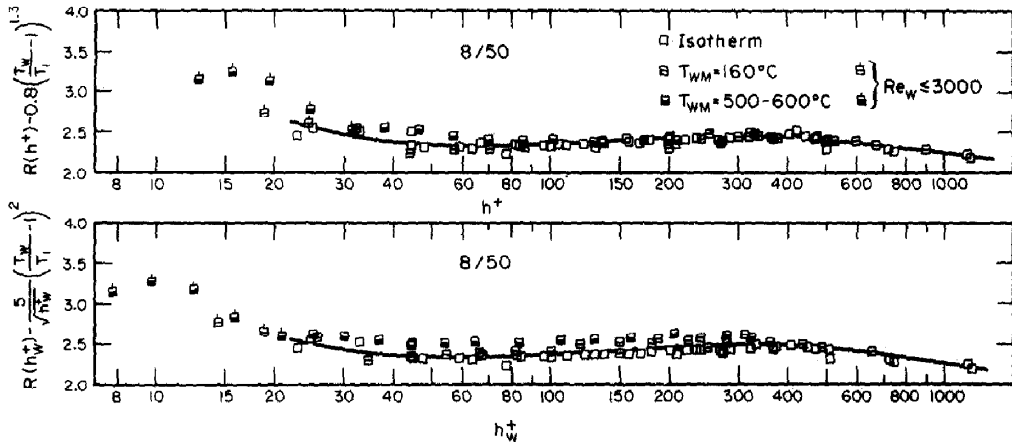


FIG. 30. $R(h^+)_1 = R(h^+) - 0.8 \left(\frac{T_w}{T_1} - 1 \right)^{1.3}$ vs h^+ , and $R(h_w^+)_1 = R(h_w^+) - \frac{5}{(h_w^+)^{1/4}} \left(\frac{T_w}{T_1} - 1 \right)^2$ vs h_w^+ for test section 8/50.

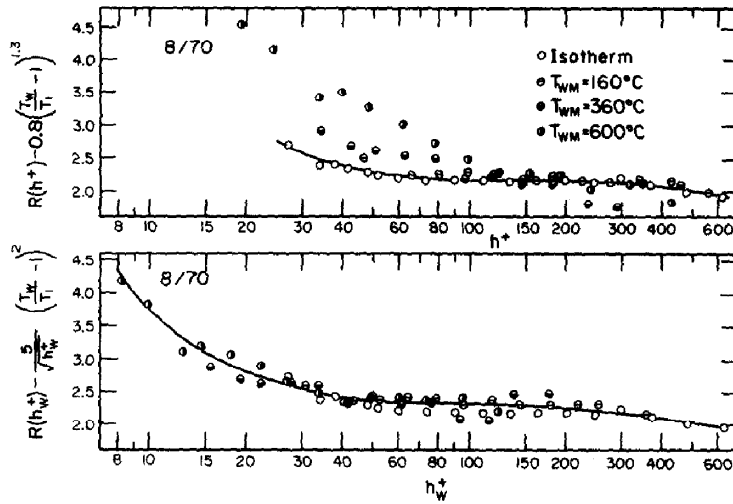


FIG. 31. $R(h^+)_1 = R(h^+) - 0.8 \left(\frac{T_w}{T_1} - 1 \right)^{1.3}$ vs h^+ , and $R(h_w^+)_1 = R(h_w^+) - \frac{5}{(h_w^+)^{1/4}} \left(\frac{T_w}{T_1} - 1 \right)^2$ vs h_w^+ for test section 8/70.

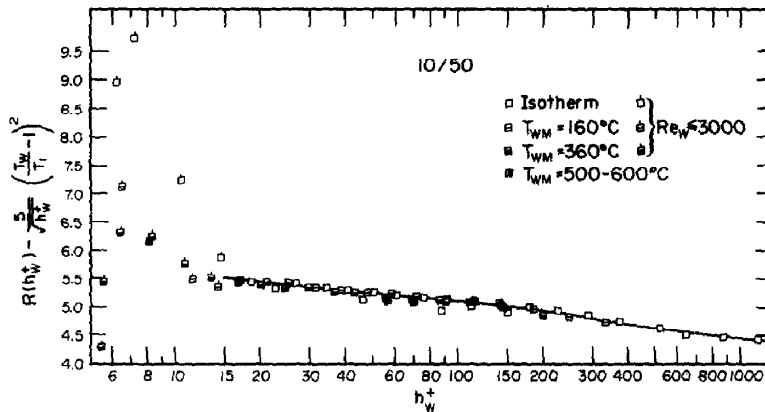


FIG. 32. $R(h_w^+)_1 = R(h_w^+) - \frac{5}{(h_w^+)^{1/4}} \left(\frac{T_w}{T_1} - 1 \right)^2$ vs h_w^+ for test section 10/50.

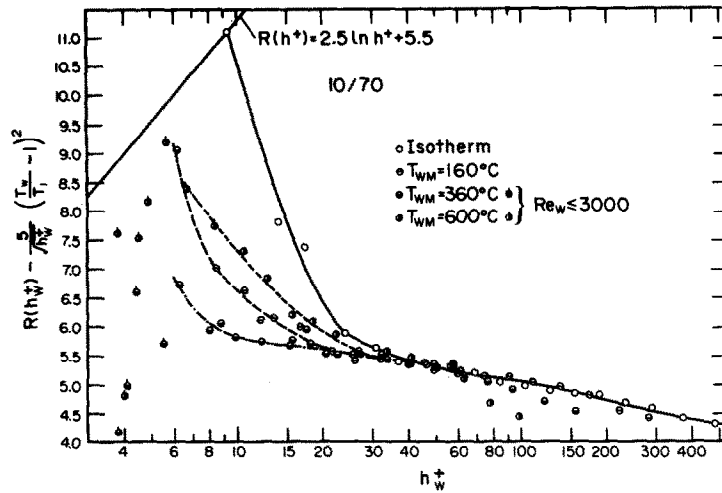


FIG. 33. $R(h_w^+)_t = R(h_w^+) - \frac{5}{(h_w^+)^2} \left(\frac{T_w}{T_1} - 1 \right)^2$ vs h_w^+ for test section 10/70.

Figures 34 and 35 show the parameter

$$GPRO1 = G(h_w^+) \left[Pr^{0.44} (T_w/T_B)^{0.5} \times \left(\frac{h}{0.01(r_2 - r_1)} \right)^{0.053} \right] \quad (80)$$

vs h_w^+ for the rods 8 and 10 respectively. As explained in more detail in [2] the parameters $(T_w/T_B)^{0.5}$ and $[h/0.01(r_2 - r_1)]^{0.053}$ are correction factors which take account of the temperature effect and of the effect of the roughness rib height in relation to the length of the temperature profile, in the same way as the ratios T_w/T_1 and h/δ take into account the temperature effect

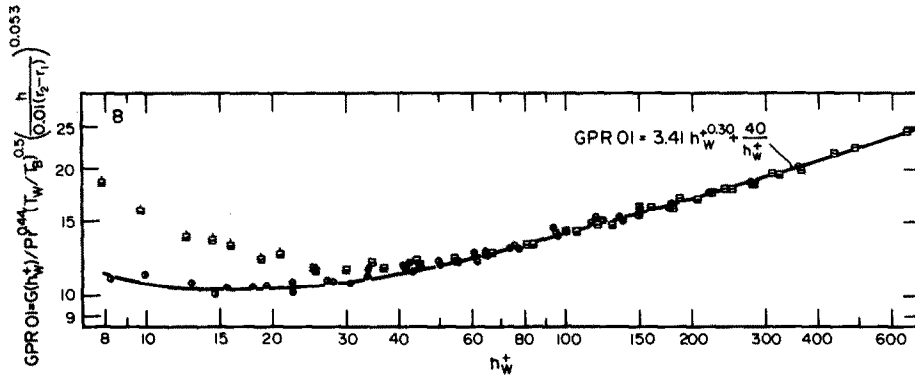


FIG. 34. $GPRO1 = G(h_w^+) \left[Pr^{0.44} (T_w/T_B)^{0.5} \left(\frac{h}{0.01(r_2 - r_1)} \right)^{0.053} \right]$ vs h_w^+ for the rough rod number 8. (Symbols of Figs. 20 and 21.)

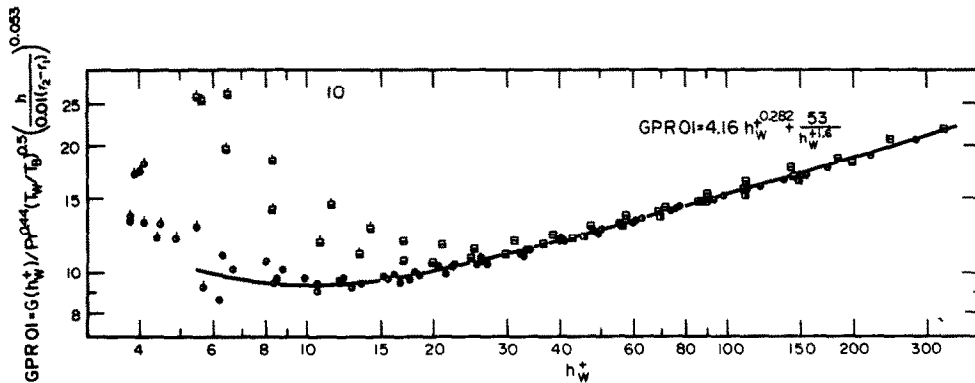


FIG. 35. $GPRO1 = G(h_w^+) \left[Pr^{0.44} (T_w/T_B)^{0.5} \left(\frac{h}{0.01(r_2 - r_1)} \right)^{0.053} \right]$ vs h_w^+ for the rough rod number 10. (Symbols of Figs. 22 and 23.)

and the effect of the rib height to the length of the velocity profile on $R(h^+)$. Due to the fact that the temperature profile is assumed to be extending over the whole of the annulus from the rough inner rod up to the adiabatic outer smooth surface, T_B and $r_2 - r_1$ are respectively used in place of T_1 and \hat{y} , which refer to the inner region of the annulus (up to the line of zero shear) only. The points in Figs. 34 and 35 represent all the heat-transfer data obtained during the present experiment, for both the rods 8 and 10, each of them in a 50 and 70 mm outer smooth tube. The points can be correlated by a single line even in the transition region between fully rough and hydraulically smooth flow, provided that $Re_w > 3000$, that is only in turbulent flow. The points for $Re_w \leq 3000$ lay considerably above the line valid for turbulent flow. This is not surprising, since the temperature profile is not logarithmic with the constant slope 2.5 in the laminar, and in the transition flow region between laminar and turbulent and, like $R(h^+)$, $G(h^+)$ doesn't have a real physical meaning for $Re_w \leq 3000$.

The data of Fig. 34 for the rod number 8 can be correlated by the expression:

$$\text{GPRO1} = 3.41(h_w^+)^{0.30} + \frac{40}{h_w^+}$$

in the range $8 \leq h_w \leq 800$ (81)

and the data of Fig. 35 for the rod number 10 by the expression:

$$\text{GPRO1} = 4.16(h_w^+)^{0.282} + \frac{53}{(h_w^+)^{1.6}}$$

in the range $5.5 \leq h_w \leq 350$. (82)

The first term on the right side of the equations (81) and (82) is the preponderant one in regions of high values of h_w^+ , that is in the region of fully rough flow, where $R(h^+)$ is quasi-constant. The second term on the right side of the equations (81) and (82) is the preponderant one in the region of low values of h_w^+ , i.e. in the transition region between fully rough and hydraulically smooth flow. In this region the reduced values of $G(h_w^+)$ appear to be more or less constant as was already found by Dipprey and Sabersky for the sand roughness [18] and by Webb for the flow inside tubes with rectangular roughness ribs [58].

The difference between equation (81) and equation (82) is not great, but it is significant. These equations confirm the finding of Dalle Donne and Meerwald that the exponent of h_w^+ for the term preponderant in the fully rough flow is higher for a roughness having lower fully rough values of $R(h^+)$. (cfr. equation (64) derived from [51]).

4.5. Main results of the present experiment

The main results of the present experiment can be summarized as follows:

1. A new transformation method, both for friction and heat-transfer coefficients has been developed, to obtain turbulent flow data applicable to other coolant channel shapes or other "macroscopic geometries" than the annulus with an inner rough rod and an

outer smooth channel, for which the experimental data are generally obtained.

This method is based on the parameter $R(h^+)$ of the universal logarithmic velocity profile introduced by Nikuradse:

$$u^+ = 2.5 \ln \frac{y}{h} + R(h^+)$$

and on the parameter $G(h^+)$ of the logarithmic temperature profile introduced by Dipprey and Sabersky:

$$t^+ = 2.5 \ln \frac{y}{h} + G(h^+)$$

and valid for turbulent Prandtl numbers near unity.

2. The parameters $R(h^+)$ and $G(h^+)$ are not completely independent of the macroscopic geometry which delimits the flow of the gas, but they are a function of the ratios of the roughness rib height to the length of the velocity and of the temperature profiles respectively.

3. The results of the present experiment prove that, for roughnesses formed by repeated ribs with a rectangular profile in the fully rough flow regime, the effect of this ratio h/\hat{y} on the parameter $R(h^+)$ is given by:

$$R(h^+) = R(h^+)_{01} + 0.4 \ln \left(\frac{h/\hat{y}}{0.01} \right)$$

so that the Nikuradse universal velocity profile can be written as follows:

$$u^+ = 2.5 \ln \left(\frac{y}{h^{0.84} y^{0.16}} \right) + R(h^+)_{01} + 1.84.$$

4. In presence of heat transfer and large temperature differences in the gas field the Reynolds number based on the roughness rib height h_w^+ should be calculated with the gas properties evaluated at the rough surface temperature, thus indicating that the phenomena occurring at the rough surface play a decisive role on the production of the turbulence, which is responsible for the transmission of both momentum and heat in radial direction.

Further correction parameters, functions of the ratio of the absolute wall temperature to the gas temperature averaged in the regions up to the zero shear surface or up to the adiabatic surface respectively, have been obtained, which correlate the $R(h^+)$ values in the fully rough flow region and the $G(h^+)$ values in the whole turbulent flow region investigated in the present experiment.

5. For low h_w^+ values the $R(h^+)$ data fall on the line:

$$R(h^+) = 2.5 \ln y^+ + 5.5$$

predicted by Nikuradse for hydraulically smooth turbulent flow, provided that $Re_w > 3000$.

6. For $Re_w \leq 1800$ the friction data agree very well with the theoretical prediction of Tiedt for the laminar flow in concentric smooth annuli, and with the temperature effect obtained by Dalle Donne and Bowditch for the laminar flow of gases inside tubes at high temperatures.

7. The heat-transfer data in turbulent flow regime ($Re_w > 3000$) can be correlated in terms of the ratio:

$$GPRO1 = G(h_w^+) \left/ \left[Pr^{0.44} (T_w/T_B)^{0.5} \times \left(\frac{h}{0.01(r_2 - r_1)} \right)^{0.053} \right] \right.$$

for all the four test sections investigated, which are typical of a roughness with low $R(h^+)$ values (high friction factors) and of a roughness with high $R(h^+)$ values (low friction factors), both in a large and in a small outer smooth channel.

8. The heat-transfer data for the roughness with low $R(h^+)$ values are correlated by the expression:

$$GPRO1 = 3.41(h_w^+)^{0.30} + \frac{40}{h_w^+} \text{ for } 8 \leq h_w \leq 800$$

and the heat-transfer data for the roughness with high $R(h^+)$ values by the expression:

$$GPRO1 = 4.16(h_w^+)^{0.282} + \frac{53}{(h_w^+)^{1.6}} \text{ for } 5.5 \leq h_w \leq 350.$$

These expressions have a form similar to that of the curves obtained by Dipprey and Sabersky and by Webb for flow in tubes and for small temperature differences between surface and coolant (constant physical properties in the coolant field). The differences in our two expressions are small but still significant. They confirm the finding of Dalle Donne and Meerwald that the exponent of h_w^+ for the factor preponderant in the region of fully rough flow (the first factor on the right side of the two expressions) is higher for roughnesses having lower values of $R(h^+)$.

5. THE DATA FROM THE LITERATURE TRANSFORMED WITH THE PRESENT METHOD

5.1. Friction data

Table 2 shows the geometrical characteristics of roughnesses with ribs with rectangular profile investigated by various authors from the literature. Table 2 shows also their friction data in terms of $R(h_w^+)$. The values of $R(\infty)$ of Table 2 are averages of the experimental data of these various authors for $h_w^+ \geq 70$. In this region of h_w^+ the values of $R(h_w^+)$ remain more or less constant and independent of h_w^+ (region of fully rough flow).

Table 2.

Reference	Author	Year	Geometry	Roughness parameters			$R(\infty)$	$R(\infty)_{01}$	Symbol
				$\frac{p-b}{h}$	h/b	h/\hat{y}			
[62]	Möbius	1940	Tube	9.00	1.00	0.101	3.54	2.61	◻
				9.03	1.00	0.101	3.54	2.61	
				18.0	1.00	0.101	4.25	3.33	
				18.5	1.00	0.100	4.13	3.21	
				36.0	1.00	0.100	5.33	4.41	
				30.2	0.60	0.060	6.38	5.66	
				8.2	2.20	0.222	2.93	1.69	
				60.6	0.30	0.030	10.6	10.2	
				28.5	0.99	0.140	4.61	3.55	
				18.0	1.00	0.060	4.45	3.73	
				18.6	0.97	0.029	4.99	4.57	
				18.3	0.98	0.039	4.67	4.13	
				[15]	Chu-Streeter	1949	Tube	1.03	
1.02	0.93	0.022	11.8					11.5	
1.02	0.93	0.039	13.5					13.0	
3.02	0.93	0.022	5.08					4.80	
7.06	0.93	0.022	3.37					3.09	
[16]	Sams	1952	Tube	0.73	1.37	0.025	7.20	6.83	◻
				1.16	1.12	0.037	9.20	8.68	
				1.14	0.88	0.016	11.90	11.70	
[17]	Nunner	1956	Tube	19.20	0.80	0.080	4.53	3.68	◻
[63]	Koch	1958	Tube	8.80	1.00	0.081	3.81	2.96	◻
				18.6	1.00	0.080	4.75	3.90	
				77.4	1.00	0.080	8.16	7.31	
				155.8	1.00	0.080	10.60	9.79	
				3.72	5.00	0.202	3.59	2.38	
				9.60	5.00	0.201	3.21	2.00	
				64.80	5.00	0.200	5.75	4.54	
				195.80	5.00	0.200	9.30	8.09	
				[64]	Fedynskii	1959	Annulus	5.67	
12.30	1.00	0.104	3.00					2.06	
15.7	1.00	0.106	3.20					2.25	

Table 2.—Continued





Reference	Author	Year	Geometry	Roughness parameters					Symbol
				$\frac{p-b}{h}$	h/b	h/\bar{y}	$R(\infty)$	$R(\infty)_{01}$	
[65]	Draycott, Lawther	1961	Annulus	1.00	1.00	0.130	11.00	9.92	☐
				1.00	1.00	0.066	9.33	8.57	
				1.00	1.00	0.045	8.93	8.33	
				1.00	1.00	0.035	8.62	8.13	
[66]	Skupinski	1961	Annulus	1.00	1.00	0.208	9.21	8.00	☐
				2.00	1.00	0.188	6.60	5.42	
				10.00	1.00	0.158	3.02	1.92	
				20.00	1.00	0.167	4.59	3.46	
			Tube	40.00	1.00	0.179	6.29	5.14	
				66.20	2.00	0.200	6.41	5.21	
				39.50	2.00	0.200	5.15	3.96	
				21.70	2.00	0.201	4.18	2.98	
[67]	Savage, Myers	1963	Tube	10.60	2.00	0.202	3.47	2.27	☐
				16.00	2.67	0.166	3.27	2.15	
				6.00	2.67	0.166	3.00	1.87	
				2.00	2.67	0.169	4.12	2.99	
				1.00	2.67	0.172	5.05	3.91	
				12.00	1.33	0.083	3.23	2.38	
				8.00	1.33	0.083	3.11	2.26	
				4.00	1.33	0.083	3.49	2.64	
[68]	Sheriff, Gumley, France	1963	Annulus	2.00	1.33	0.084	4.47	3.61	☐
				9.00	1.00	0.028	3.07	2.64	
				4.00	1.00	0.030	4.41	3.96	
				1.00	1.00	0.079	12.50	11.70	
[69]	Gargaud, Paumard	1964	Tube	1.00	1.00	0.040	9.88	9.32	☐
				9.00	1.00	0.020	3.40	3.13	
				9.00	1.00	0.031	3.19	2.74	
				6.00	1.00	0.008	2.66	2.75	
				9.00	1.00	0.008	3.98	4.07	
				14.00	1.00	0.008	4.29	4.38	
				4.00	1.00	0.012	3.72	3.65	
				6.00	1.00	0.012	3.53	3.46	
			Annulus	14.00	1.00	0.012	4.72	4.66	
				2.00	1.67	0.020	7.01	6.73	
				3.00	1.67	0.020	3.87	3.60	
				4.00	1.67	0.020	3.25	2.98	
				0.50	1.60	0.031	10.60	10.10	
				1.00	1.60	0.031	10.90	10.50	
				2.00	1.60	0.031	6.55	6.10	
				9.00	1.00	0.060	3.39	2.67	
[70]	Massey	1966	Annulus	15.00	1.00	0.064	3.99	3.20	☐
				14.60	1.00	0.096	3.80	2.85	
				15.00	1.00	0.116	3.76	2.74	
				6.16	1.06	0.100	2.32	1.39	
				6.16	1.06	0.192	2.71	1.53	
[70]	Massey	1966	Annulus	13.30	1.06	0.103	3.04	2.11	☐
				13.30	1.06	0.196	3.63	2.44	
				27.50	1.06	0.112	5.13	4.17	
				27.50	1.06	0.215	6.03	4.80	

Before obtaining the $R(h_w^+)$ values, the experimental friction factors from the literature were always reduced to the same definition of hydraulic diameter. In the literature it is possible to find three different definitions of hydraulic diameter. One based on the tips of the roughness ribs, one on the root of the ribs, the third on the "volumetric" diameter of the rough surface, i.e. on the diameter of the surface which one would obtain by smearing the rib on the surface itself. This seems to be the most appropriate definition, because the

Nikuradse's law of the wall [equation (2)] is obviously referred to a velocity profile averaged in axial direction over the pitch of the roughness ribs p . This is the reason why Nikuradse and Schlichting used this definition. We reduced therefore all the data from the literature given in Table 2 to the volumetric hydraulic diameter definition. Of course also the data obtained with the present experiment are based on the volumetric hydraulic diameter.

The values of $R(h_w^+)$ for the calculation of the $R(\infty)$

Table 2.—Continued

Reference	Author	Year	Geometry	Roughness parameters			$R(\infty)$	$R(\infty)_{01}$	Symbol
				$\frac{p-b}{h}$	h/b	h/\bar{y}			
[71]	Kjellström, Larsson	1967	Annulus	3.35	1.72	0.021	3.52	3.08	
				7.10	0.87	0.019	2.32	1.91	
				13.90	0.50	0.021	3.86	3.41	
				7.54	0.92	0.035	2.67	2.05	
				13.60	0.55	0.036	3.83	3.19	
				24.20	0.31	0.023	5.93	5.43	
				11.90	0.086	0.027	6.59	6.04	
				13.70	0.26	0.022	4.89	4.41	
				7.47	0.97	0.051	2.43	1.69	
				3.51	1.98	0.031	2.69	2.11	
				1.58	3.77	0.035	6.64	6.00	
				1.60	4.08	0.025	6.54	6.02	
				26.80	1.04	0.022	5.80	5.32	
				4.97	0.34	0.043	6.45	5.74	
[72]	Feurstein, Rampf	1969	Annulus	0.77	2.50	0.156	9.01	7.87	
				1.27	2.50	0.149	7.97	6.85	
				2.10	2.50	0.133	4.84	3.77	
				2.93	2.50	0.128	3.89	2.83	
				6.27	2.50	0.121	2.40	1.37	
				1.15	1.67	0.108	9.10	8.10	
				1.90	1.67	0.097	6.53	5.58	
				3.15	1.67	0.087	3.96	3.06	
				4.40	1.67	0.084	3.04	2.15	
				9.40	1.67	0.083	2.69	1.80	
				14.40	1.67	0.084	3.13	2.24	
				2.30	0.83	0.051	6.51	5.80	
				3.80	0.83	0.046	4.29	3.62	
				8.80	0.83	0.044	2.91	2.27	
				18.80	0.83	0.046	3.99	3.33	
				28.80	0.83	0.048	5.29	4.61	
4.60	0.42	0.024	4.35	3.93					
7.60	0.42	0.023	3.08	2.68					
17.60	0.42	0.024	4.73	4.01					
37.60	0.42	0.026	6.55	6.09					
[35]	Lawn, Hamlin	1969	Annulus	6.21	1.00	0.055	3.34	2.66	
[28]	Watson	1970	Annulus	5.49	1.00	0.056	2.45	1.76	
				6.19	1.00	0.035	2.55	2.05	
				6.22	1.00	0.024	2.26	1.91	
6.19	1.00	0.037	3.02	2.50					
[36]	Stephens	1970	Annulus	6.20	1.00	0.046	3.10	2.50	
[61]	Webb, Eckert, Goldstein	1971	Tube	8.97	0.97	0.020	3.69	3.40	
				9.48	1.94	0.040	3.18	2.61	
				9.74	3.88	0.080	3.15	2.31	
				19.50	1.94	0.040	4.38	3.81	
39.50	1.94	0.040	6.46	5.89					

of Table 2 have been obtained from the geometrical parameters and the reduced friction factors always by integration of Nikuradse's law of the wall [equation (2)]. Thus for flow of fluids inside rough tubes, the $R(h/\bar{y})$'s were obtained from the measured friction factors by means of the friction similarity law of Nikuradse [equation (9)], while for flow in annuli the present transformation method was used (see Section 3.6). This was done even in the cases where the velocity profiles were measured directly. For instance Lawn

and Hamlin [35] performed velocity measurements in an annulus, thus obtaining by direct measurement a value of $R(\infty)$ which differed only slightly from that obtained from the present method, shown in Table 2 [$R(\infty) = 3.34$, while the value directly measured by Lawn and Hamlin was equal to 3.57], the difference being given by the slightly different slope from 2.5 in the velocity profile found by Lawn and Hamlin (slope = 2.22). In our opinion these differences are well within the accuracy of the experiments of reference [35].

Table 2. shows the values $R(\infty)_{01}$ as well, which have been obtained from the corresponding values of $R(\infty)$ and reduced to the value $h/\hat{y} = 0.01$ and $T_w/T_B = 1$ by means of equation (72) and (78) respectively. In this, we assume that the h/\hat{y} and T_w/T_B effects on $R(\infty)$ for the roughnesses with rectangular ribs in the literature, are the same as those which were found for the roughnesses investigated by us during the present experiment. The validity of equation (72) is limited to the range $h/\hat{y} \leq 0.235$, therefore we considered from the literature only the cases where this condition was satisfied. Table 2 lists the experimental data for $h/\hat{y} \leq 0.235$ only.

the ribs and less on the flow pattern on the top face of the rib, and this is the reason why $(p-b)/h$ is a better parameter than p/h . Extending this reasoning, it is possible to understand why $R(\infty)_{01}$ presents a minimum for $(p-b)/h \approx 6$ in Fig. 36. For $(p-b)/h$ greater than 6 the region of the wall, where the viscous layer is growing and the local friction factors decrease, increases when $(p-b)/h$ increases, therefore the total friction factor decreases too and $R(\infty)_{01}$ increases. On the other hand for $(p-b)/h$ smaller than 6 the vortex behind the rib occupies always more of the space between two adjacent ribs as $(p-b)/h$ decreases.

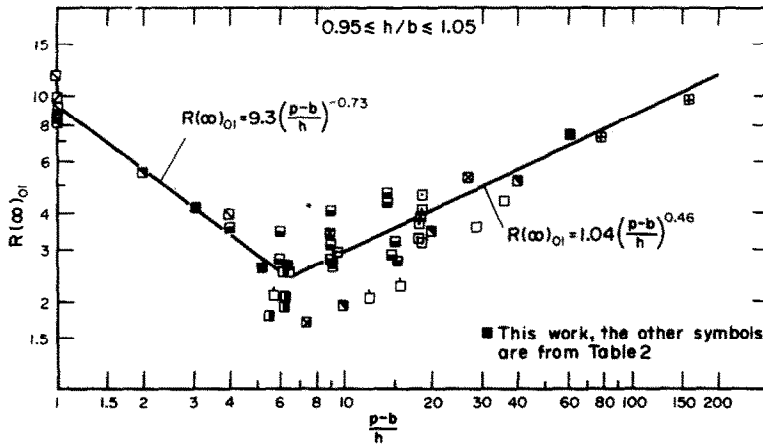


FIG. 36. $R(\infty)_{01}$ vs $(p-b)/h$ for $0.95 \leq h/b \leq 1.05$.

Figure 36 shows the values of $R(\infty)_{01}$ for rectangular ribs with $0.95 \leq h/b \leq 1.05$ vs $(p-b)/h$ from the present experiment [the values of $R(\infty)_{01}$ for the present experiment, shown in graphs with black squares are listed in Table 1] and from the various authors of Table 2. To try to simplify the correlation, we have used the parameter $(p-b)/h$ rather than p/h used previously by Dalle Donne and Meerwald [51] and Baumann and Rehme [55]. Indeed Baumann and Rehme find that in the diagram $R(\infty)$ vs p/h the position of minimum $R(\infty)$ is a function of h/b , namely it is shifted toward smaller values of p/h for higher values of h/b [55]. Obviously this effect can be, at least in part, compensated by the choice of the parameter $(p-b)/h$ rather than p/h , in such a way that the minimum of $R(\infty)$ occurs always at the same value of $(p-b)/h$, whatever is the value of h/b . This has an effect that the correlation of the data becomes much simpler. Already Kjellström [73] noticed that the parameter $(p-b)/h$ is more significant than p/h for correlating the friction data of rough surfaces. The physical explanation of this is quite simple. As Kattchee and Mackewicz [74] observed, after a rectangular rib the flow reattaches at a distance of about $x = 4h$ after the rib, the region $0 < x < 4h$ near the wall being occupied by a vortex. For $x > 4h$ the viscous layer at the wall starts to grow, therefore the local friction coefficient, which has a maximum at the point of reattachment, decreases as x increases beyond $4h$. All this is mainly dependent on what happens between

For $(p-b)/h = 2$, "a standing vortex is formed between the ribs filling approximately two thirds of the cavity. The energy interchange with the mainstream appears to be only sufficient to produce vortex shedding occasionally" [75]. The flow becomes more and more a "quasi-smooth flow" [76], as the frequency of the vortex shedding decreases with the decreasing of $(p-b)/h$. Thus for $(p-b)/h < 6$ the friction factor decreases when $(p-b)/h$ decreases. In the region $(p-b)/h \approx 6$ the friction factor has thus a maximum, and $R(\infty)_{01}$ consequently a minimum.

The data of Fig. 36 can be correlated by:

$$R(\infty)_{01} = 9.3 \left(\frac{p-b}{h} \right)^{-0.73} \pm 1 \text{ for } 1 \leq \frac{p-b}{h} \leq 6.3$$

$$0.95 \leq \frac{h}{b} \leq 1.05 \quad (83)$$

and

$$R(\infty)_{01} = 1.04 \left(\frac{p-b}{h} \right)^{0.46} \pm 1 \text{ for } 6.3 \leq \frac{p-b}{h} \leq 160$$

$$0.95 \leq \frac{h}{b} \leq 1.05. \quad (84)$$

The scatter of ± 1 , which implies a scatter in the transformed friction factors of about $\pm 15\%$, is rather large and can be explained by the fact that the points derive from many different experiments, in different laboratories, over a period of time of over thirty years. Geometrical tolerances, both of the roughness ribs and of the channels which contained the roughness surfaces,

as well as rounding of the ribs given by various fabrication processes, may produce a considerable scatter in the value of $R(\infty)_{01}$ [31]. Another possible cause of scatter of the values of the roughness parameters is the fact that the $R(h_w^+)_{01}$ values are not exactly constant for $h_w^+ > 70$, thus the averaging performed to obtain $R(\infty)$ may have produced scattering of the values, as the $R(h_w^+)$ were obtained by the various authors in different ranges of h_w^+ . It should be noticed however that the scatter of the points obtained in the present experiment (black squares) is considerably less than that of the others.

been eliminated, the scatter of the points being more or less the same as in Fig. 36. Thus one can conclude that all the data of Table 2 and from the present experiment, which cover the range:

$$\begin{aligned} 1 &\leq \frac{p-b}{h} \leq 160 \\ 0.086 &\leq \frac{h}{b} \leq 5.0 \\ 0.008 &\leq \frac{h}{y} \leq 0.235 \end{aligned} \tag{85}$$

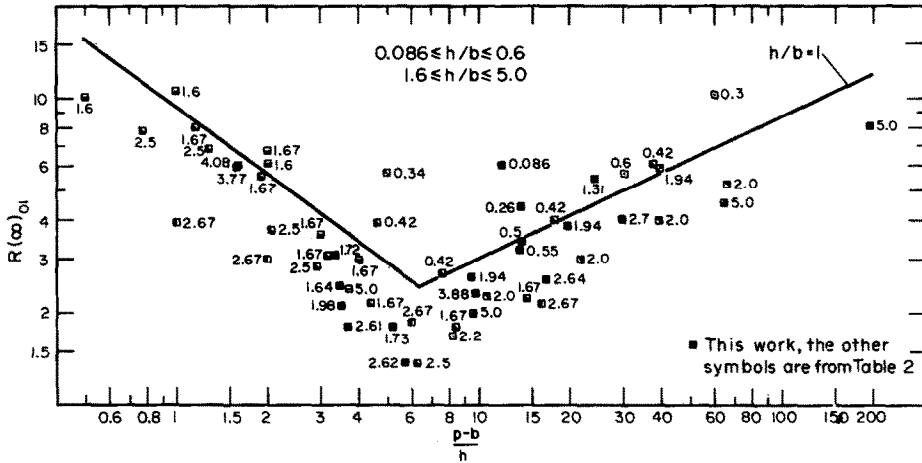


FIG. 37. $R(\infty)_{01}$ vs $(p-b)/h$ for $0.086 \leq h/b \leq 0.6$ and $1.6 \leq h/b \leq 5.0$. (The numbers beside the points indicate the value of h/b .)

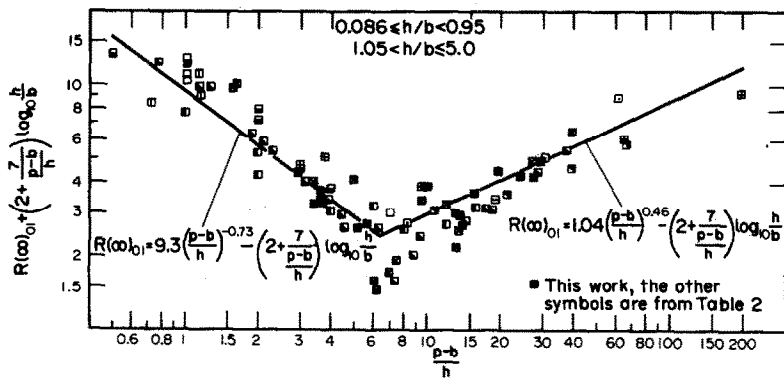


FIG. 38. $R(\infty)_{01} + [2 + 7[(p-b)/h]] \log_{10}(h/b)$ vs $(p-b)/h$ for $0.086 \leq h/b < 0.95$ and $1.05 < h/b \leq 5.0$.

Figure 37 shows the values of $R(\infty)_{01}$ vs $(p-b)/h$ for h/b different from unity ($0.086 \leq h/b \leq 0.6$, $1.6 \leq h/b \leq 5.0$), each point having its h/b value indicated near the symbol. A systematic h/b effect greater than the scattering of the points is quite evident over the whole range of $(p-b)/h$. Figure 38 shows the same points and the others for $0.6 < h/b < 0.95$ and $1.05 < h/b < 1.6$ in the diagram

$$R(\infty)_{01} + \left[2 + \frac{7}{(p-b)/h} \right] \log_{10} \frac{h}{b}$$

vs $(p-b)/h$. The systematic h/b effect of Fig. 37 has

are correlated by:

$$R(\infty)_{01} = 9.3 \left(\frac{p-b}{h} \right)^{-0.73} - \left[2 + \frac{7}{(p-b)/h} \right] \log_{10} \frac{h}{b} \pm 1 \quad \text{for } 1 \leq \frac{p-b}{h} \leq 6.3 \tag{86}$$

$$R(\infty)_{01} = 1.04 \left(\frac{p-b}{h} \right)^{0.46} - \left[2 + \frac{7}{(p-b)/h} \right] \log_{10} \frac{h}{b} \pm 1 \quad \text{for } 6.3 \leq \frac{p-b}{h} \leq 160. \tag{87}$$

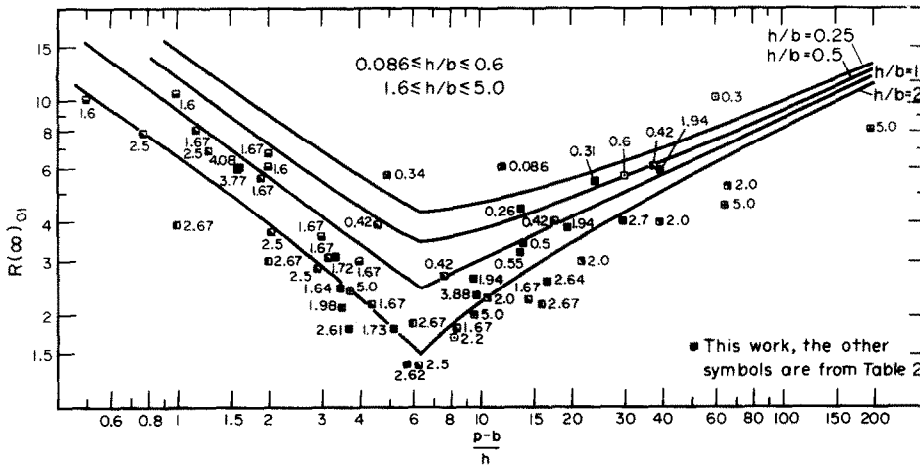


FIG. 39. $R(\infty)_{01}$ vs $(p-b)/h$ for $0.086 \leq h/b \leq 0.6$ and $1.6 \leq h/b \leq 5$. Comparison with suggested correlation. (The numbers beside the points indicate the value of h/b .)

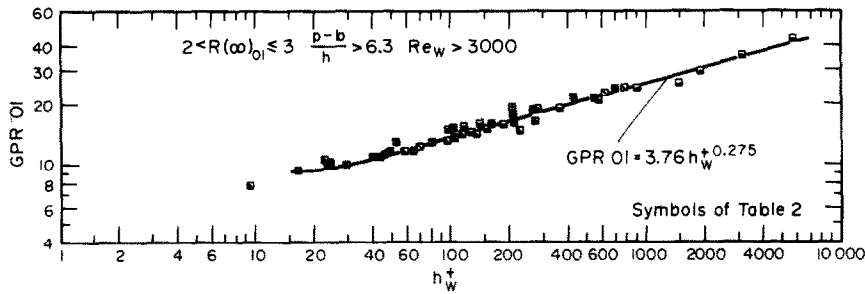


FIG. 40. GPRO1 vs h_w^+ for $2 < R(\infty)_{01} \leq 3$ and $(p-b)/h > 6.3$.

Figure 39 shows the same points of Fig. 37 in the diagram $R(\infty)_{01}$ vs $(p-b)/h$. Also equations (86) and (87) for $h/b = 0.25, 0.5, 1, 2$ are shown in the figure. One can notice that the equations suggested correlate the points tends to increase quite considerably. We $(p-b)/h$ and h/b too high or too low the scatter of the points tends to increase quite considerably. We would therefore recommend to use equations (86) and (87) not in the range (85) but in the more restricted range:

$$\begin{aligned}
 2 &\leq \frac{p-b}{h} \leq 20 \\
 0.25 &\leq \frac{h}{b} \leq 2 \\
 0.008 &\leq \frac{h}{\bar{y}} \leq 0.235.
 \end{aligned}
 \tag{88}$$

This is the most interesting range for practical purposes, because it is in this range that the thermal performance of the roughness is really higher than that of a smooth surface, as shown in [2].

5.2. Heat-transfer data

For all the papers listed in Table 2 and which reported heat-transfer measurements with gases we evaluated the function $G(h_w^+)$. In case of flow inside tubes we used the Dipprey-Sabersky relationship [equation (16)]. For flow inside annuli we used the present transformation method, whereby it was not

possible to use equation (50), because the temperature of the outer wall of the annulus was not generally available, and equation (58) was used in its place. In [2] it is shown that this does not make much difference.

The function GPRO1 was calculated by means of equation (80). In this, again, we assume that the (T_w/T_B) and $h/(r_2 - r_1)$ effects on $G(h_w^+)$ for the roughnesses with rectangular ribs of Table 2 are the same as those which were found for the roughnesses investigated by us during the present experiment.

In [2] the heat-transfer data for the papers of Table 2 have been plotted in diagrams GPRO1 vs h_w^+ . The data have been sorted out according to the relative $R(\infty)_{01}$ values and $(p-b)/h$ values (either greater or smaller than 6.3). Figure 40 shows for instance the literature data for the range $3 < R(\infty)_{01} \leq 4$ and $(p-b)/h > 6.3$. For GPRO1 > 10 the data can be correlated by an equation of the type:

$$GPRO1 = K_1 \cdot h_w^{+K_2} \tag{89}$$

as in the case of the heat-transfer data obtained during the present experiment. The scatter of the points is of course greater than in the case of our data (cf. with Figs. 34 and 35) for the same reasons, which we discussed in the previous Section 5.1 for the friction data, but no systematic trend can be observed. Only the data of Koch for $h/b = 5$ [63] are systematically higher than the others, as one can see from Fig. 40 as well as from the other graphs in [2]. This is probably due

to a so called “fin efficiency effect”, as already noticed by Dalle Donne and Meerwald [51]. With the thin ribs of Koch ($h/b = 5$) the heat-transfer coefficient is considerably decreased by the finite heat conduction along the ribs, leading to higher values of GPRO1, while lower and/or wider ribs can be practically considered at constant temperature. This effect is dealt in detail by Mantle, Freeman and Watts [77]. For $GPRO1 \leq 10$, the values of GPRO1 remain more or less constant as h_w decreases (see [2]).

trapezoidal and rectangular) while the present investigation has been restricted to roughnesses with rectangular ribs only. The scatter in the graphs of Dalle Donne and Meerwald was considerably higher, but the agreement between the present correlations and those suggested by Dalle Donne and Meerwald is surprisingly good.

6. APPLICATION TO CONDITIONS TYPICAL OF A FUEL ELEMENT OF A GAS COOLED FAST REACTOR

Once the parameters $R(h_w^+)$ and $G(h_w^+)$ are known the friction factor and the heat-transfer coefficient for the fuel elements of a gas cooled fast reactor can be calculated. These fuel elements are made up of bundles of rough rods in a regular triangular array. Generally the ratio of the pitch of the rods to the rod diameter p_r/d is greater than 1.2, thus no acute corners between surfaces are present, secondary flows play a negligible role and the logarithmic velocity distribution [equation (2)] still holds [14]. For the central coolant sub-channels of the bundle, unaffected by the subassembly walls, surrounded by rough heat-transfer surfaces only and where the condition of coincidence of zero shear stress and zero heat flux is given, it is possible to obtain the average dimensionless velocity \bar{u}^+ by the integration over y^+ of the universal velocity profile relative to rough surfaces:

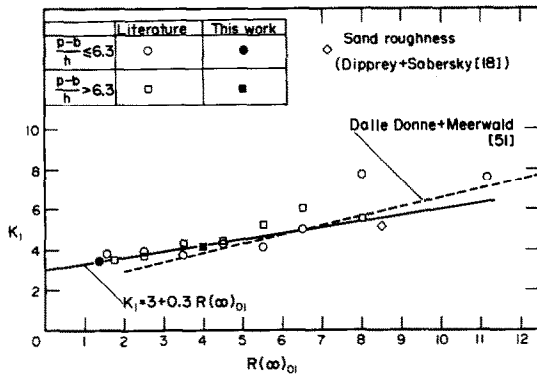


FIG. 41. Coefficient K_1 of equation (89) vs $R(\infty)_{01}$.

Figures 41 and 42 show the parameters K_1 and K_2 as defined by equation (89). Each couple of values K_1 and K_2 has been obtained by a diagram similar to that of Fig. 40 (for the other diagrams see [2]) and from the present experiment (Figs. 34 and 35). The graphs of Figs. 41 and 42 show that GPRO1 is independent of $(p - b)/h$ and it is a function of $R(\infty)_{01}$ only. The scattering of the points is considerable, but the effects on GPRO1 are smaller than it would appear at first sight from these diagrams, because to each value of K_1 lower than the correlation line is associated a value of K_2 higher than the respective correlation line and vice versa, so that these two differences compensate each other on GPRO1, at least in part. The correlating equations are:

$$K_1 = 3.0 + 0.3R(\infty)_{01} \tag{90}$$

$$K_2 = 0.32 - 0.017R(\infty)_{01} \tag{91}$$

Figures 41 and 42 show also, for comparison, the lines suggested by Dalle Donne–Meerwald [51] and valid for ribs of different shapes (circular, triangular,

$$u^+ = 2.5 \ln \frac{y}{h} + R(h_w^+) \tag{2}$$

in an equivalent annular zone having the same cross sectional area of the hexagonal area relative to a single rod of the cluster. The result of this integration is given by:

$$\bar{u}^+ = 2.5 \ln \left(\frac{p_r^* - d}{2h} \right) + R(h_w^+) - \frac{3.75 + 1.25p_r^*/d}{1 + p_r^*/d} \tag{92}$$

where $p_r^* = [2(3)^{1/2}/\pi]^{1/2} p_r$ is the diameter of the equivalent annular zone. When one considers that $\bar{u}^+ = (2/f_R)^{1/2}$, one has:

$$\left(\frac{2}{f_R} \right)^{1/2} = 2.5 \ln \left(\frac{p_r^* - d}{2h} \right) + R(h_w^+) - \frac{3.75 + 1.25p_r^*/d}{1 + p_r^*/d} \tag{93}$$

In a similar way the average dimensionless temperature \bar{t}^+ is obtained by integration of the universal temperature profile relative to rough surfaces:

$$t^+ = 2.5 \ln \frac{y}{h} + G(h_w^+) \tag{11}$$

in the same equivalent annular zone. The integration yields:

$$\bar{t}^+ = 2.5 \ln \left(\frac{p_r^* - d}{2h} \right) + G(h_w^+) - \frac{3.75 + 1.25p_r^*/d}{1 + p_r^*/d} \tag{94}$$

From equations (93) and (94) one has:

$$\bar{t}^+ = G(h_w^+) + \left(\frac{2}{f_R} \right)^{1/2} - R(h_w^+) \tag{95}$$

and remembering that $\bar{t}^+ = (f_R/2)^{1/2}/St_R$, one obtains

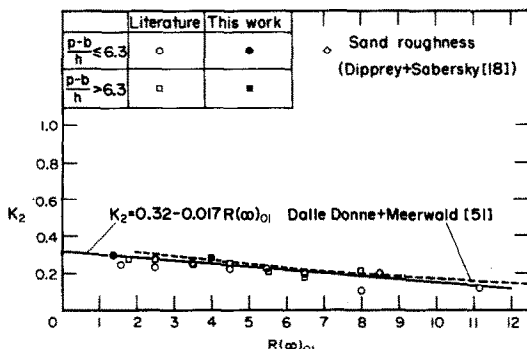


FIG. 42. Coefficient K_2 of equation (89) vs $R(\infty)_{01}$.

the Stanton number for the central rough coolant subchannels of the bundle:

$$St_R = \frac{f_R/2}{1 + (f_R/2)^2 [G(h_w^+) - R(h_w^+)]} \quad (96)$$

Considering equations (72) and (78), $R(h_w^+)$ is given by:

$$R(h_w^+) = R(\infty)_{01} + 0.4 \ln \frac{(2h/d)}{(p_r^*/d-1)} + \frac{5}{(h_w^+)^{1/2}} \left(\frac{T_w}{T_b} - 1 \right)^2 + \frac{5100}{h_w^{+3}} \quad (97)$$

where: $R(\infty)_{01}$ is given by equations (86) and (87), the term $2h/d/p_r^*/d-1$ corresponds to the ratio h/\hat{y} of the annulus, and the term $5100/h_w^{+3}$ takes into account the transition region between turbulent fully rough flow and smooth flow. This term has been obtained as an average of the values obtained for the tube 10 of the present investigation. The transition region value of $R(h_w^+)$ is probably not independent of the value of $R(\infty)_{01}$, and we have seen that it is very much affected by T_w/T_b , thus the transition term is subjected to considerable uncertainty. Further experimental work is required for the transition region, especially as far as friction data are concerned. The transition term $5100/h_w^{+3}$, however, becomes appreciable only for $h_w^+ < 30$, a region where the thermal performance of the roughness is rapidly decreasing for the conditions typical of a gas cooled fast reactor (see [2]).

Of course if the $R(h_w^+)$ value calculated with equation (97) is higher than $2.5 \ln h_w^+ + 5.5$, this means that we are in the region of turbulent smooth flow and we replace equation (97) with equation (98):

$$R(h_w^+) = 2.5 \ln h_w^+ + 5.5. \quad (98)$$

Further limiting conditions are those obtained in the present experiment:

$$\begin{aligned} Re_w &> 3000 \\ \frac{h}{\hat{y}} = \frac{2h/d}{p_r^*/d-1} &< 0.235 \\ h_w^+ &> 6. \end{aligned} \quad (99)$$

From equation (80) we obtain $G(h_w^+)$ for the bundle:

$$G(h_w^+) = GRPO1 \cdot Pr^{0.44} (T_w/T_b)^{0.5} \times \left(\frac{2h/d}{0.01(p_r^*/d-1)} \right)^{0.053} \quad (100)$$

where GPRO1 is given by equations (89)–(91). When the GPRO1 thus calculated is less than 10, then it is set equal to 10 (see [2]).

The method described above was used for the evaluation of experiments with a bundle of twelve rough rods, which have been carried out in the helium high pressure loop of the Institute of Neutron Physics and Reactor Engineering at Karlsruhe. The agreement between theoretical prediction and measurement was excellent [78] and considerably better than the agreement which one would have obtained with the previous methods based on the integral parameters f_R and St_R

and the equivalent hydraulic diameter. For instance, Walker, White and Burnett were forced to use for each subchannel of different form a different empirical equation for f_R and St_R to correlate their experimental data for a rough rod bundle [79]. Yet with the present method the values of f_R and St_R for each coolant subchannel are obtained by means of an integration of always the same velocity and temperature profiles. The resulting differences in the calculated values of f_R and St_R for the various subchannels are given merely by the effect of the different subchannel shapes on the integral.

Figures 43 and 44 show the ratio St_R/St_S vs f_R/f_S and the thermal performance $(St_R/St_S)^3/(f_R/f_S)$ vs f_R/f_S for the following conditions typical of a gas cooled fast reactor fuel element:

$$\begin{aligned} p_r/d &= 1.4 \\ \text{rib profile} &= \text{rectangular} \\ h/b &= 2 \\ Re_w &= 10^5 \\ Pr &= 0.667 \text{ (helium coolant)} \\ T_w/T_b &= 1. \end{aligned} \quad (101)$$

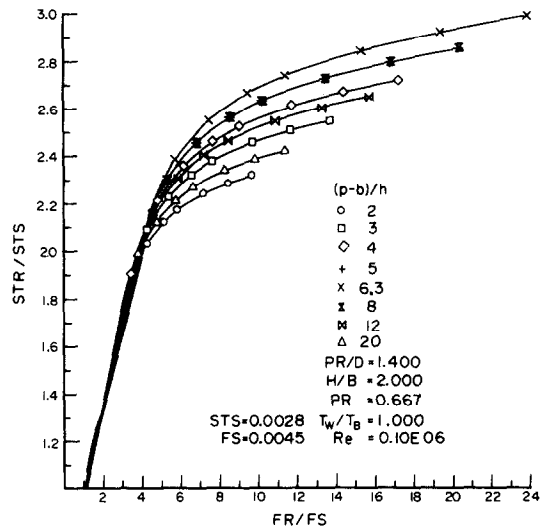


FIG. 43. Stanton vs friction multiplier for rod bundle.

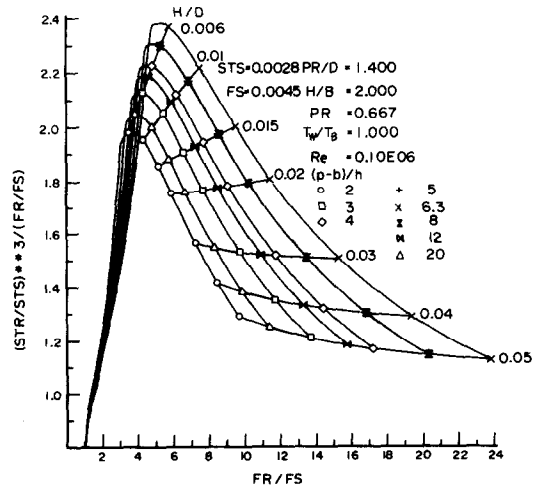


FIG. 44. Thermal performance of rod bundle.

St_S and f_S have been obtained from the equations recommended for the flow of a gas inside a smooth tube. Namely St_S from the Dalle Donne–Bowditch correlation [59] and f_S from the Prandtl–Nikuradse universal law of friction for smooth pipes [equation (36)]. Further results for $h/b = 0.25, 0.5$ and 1 are given in [2]. Figure 44 shows the improvement in the thermal performance caused by the roughness. The optimum is between 2.3 and 2.4 in the region of f_R/f_S between 4 and 6. For each value of h/d the optima are given by $(p-b)/h = 6.3$. In general one can say that as $R(h^+)$ decreases the thermal performance improves.

The “Stanton multiplier” St_R/St_S varies considerably less than the thermal performance. Typically one has a Stanton multiplier of 2 for a friction multiplier f_R/f_S equal 4.

The practical significance of the improvement in thermal performance is illustrated by the following equation derived in [2]:

$$\frac{Q}{N} = \frac{2\eta(T_w - T_m)^3}{q^2} \rho \cdot \bar{\rho} c_p^3 \frac{St_R^3}{f_R} \quad (102)$$

where: Q = reactor thermal power; N = pumping power required to circulate the coolant gas through the “rough region” of the reactor; η = efficiency of the blower; $T_w - T_m$ = temperature difference between fuel element surface and coolant gas; q = heat flux at the fuel element surface; ρ_1 = gas density at the blower; $\bar{\rho}$ = average gas density in the reactor; c_p = specific heat of the gas coolant.

If the pumping power were given by the pressure drop in the rough region of the reactor only, an improvement of the thermal performance St_R^3/f_R of the factor 2.3 would entail, according to equation (102), either an increase of the heat flux of 50%, or a reduction of the gas pressure to 2/3, or a reduction of the temperature difference to 3/4, or a reduction of the pumping power to 44%.

7. CONCLUSIONS

The experiments to measure the heat transfer and friction coefficients from rough surfaces are generally performed with a single heated rough rod contained in a concentric smooth tube, although the reactor fuel elements are made up of a number of parallel fuel pins placed in regular arrays and cooled by gas flowing parallel to the pins. The authors have developed a new method of transforming the experimental results obtained with a single rod so that they can be applied to reactor fuel elements.

The method is based on the assumption that the velocity and temperature profiles normal to the rough surface can be described in turbulent flow by the universal laws of the wall:

$$u^+ = 2.5 \ln \frac{y}{h} + R(h^+)$$

$$t^+ = 2.5 \ln \frac{y}{h} + G(h^+)$$

where u^+ and t^+ are the dimensionless velocity and temperature at the distance y from the rough wall,

h is the height of the ribs of the roughness, and $R(h^+)$ and $G(h^+)$ are the dimensionless velocity and temperature at the point $y = h$, i.e. at the tip of the ribs. In this assumption it is implicit that the parameters, which have influence on the velocity and temperature profiles, i.e. on the friction and heat transfer coefficients, do so through the quantities $R(h^+)$ and $G(h^+)$ only.

For the transformation of the friction factors the cross section of the annulus is divided into two regions, the inner one pertaining to the rough inner rod, the outer one to the outer smooth tube. The separation line is given by the line of no shear. As in the Maubach method, it is assumed that this separation line is determined by the intersection of the two velocity profiles starting from the inner rough rod and from the outer smooth surface respectively. In the present method, however, the slope A_S of the velocity profile relative to the smooth wall is assumed to be a function of the friction factor of the inner rough rod, to take into account a larger amount of experimental information on the position of the zero shear stress line.

For the transformation of the heat-transfer coefficients it is assumed that the above mentioned universal temperature profile holds over the whole cross section of the annulus from the inner rough surface over the line of zero shear up to the outer smooth surface, which is taken to coincide with the surface of zero heat flux. $G(h^+)$ is determined by the measurement of the temperatures of the two walls of the annulus. In this way we obtain a temperature profile with well defined boundary conditions (q_1 = heat flux at the rough wall, q_2 = heat flux at the smooth wall = 0), which correspond to those of the central coolant subchannels of rough clusters of rods.

The present transformation method of the friction factors agrees very well with the results of experiments performed by Wilson, who measured the shear stress on the rough inner surface of an annulus directly by means of weighing [43]. Furthermore the values of $R(h^+)$ and $G(h^+)$ obtained with the present transformation method from our measurements in annuli at low temperature, agree well with the data of Webb [58]. The data of Webb, being obtained for flow inside completely rough tubes at low temperatures, do not need any transformation and, again, the good agreement confirms our transformation method both for the friction and the heat-transfer coefficients.

During the present experiment, friction factors have been measured of ten different rough rods with two-dimensional rectangular ribs, each rod being tested subsequently in four different outer smooth tubes. Furthermore heat-transfer coefficients have been measured for two of these rods, each subsequently in two different outer smooth tubes. From these measurements the effects of three dimensionless groups (Reynolds number based on the roughness height and on the gas properties evaluated at the wall temperature, ratio of the roughness height to the length of the velocity or temperature profile, ratio of the wall temperature to the gas bulk temperature) have been found

on the velocity and temperature profiles of the fluid in turbulent flow. The data from the literature for roughness with two-dimensional rectangular ribs have been transformed with the present method. In this way the effect of the additional determining parameters was established, that is the effect of the microscopic geometrical parameters characterizing the rectangular ribs, in a range particularly interesting for practical purposes.

The present transformation method has been applied to a geometrical configuration typical of a fuel element of a gas cooled fast reactor. In this it was assumed that the velocity and temperature profiles in cross sections of the coolant subchannels of the bundle are given by the logarithmic expressions shown above. The parameters $R(h^+)$ and $G(h^+)$ and the effect of the determining parameters mentioned above are considered as invariant in the transformation from annulus to bundle geometry. By integration of the velocity and temperature profiles in the coolant subchannels the average values \bar{u}^+ and \bar{t}^+ of these profiles are obtained. These average values are directly connected with the friction factors and Stanton numbers through the expressions:

$$\bar{u}^+ = (2/f_R)^{\frac{1}{2}}$$

$$\bar{t}^+ = (2/f_R)^{\frac{1}{2}}/St_R.$$

In this way the values of f_R and St_R and the ratio St_R^3/f_R (thermal performance of the roughness) of a bundle of rods can be calculated.

The method described above was used for the evaluation of experiments with a bundle of twelve rough rods. The agreement between theoretical prediction and measurement was excellent [78] and considerably better than the agreement which one would have obtained with the previous methods based on the integral parameters f_R and St_R and the equivalent hydraulic diameter.

Acknowledgements—The authors wish to thank Prof. Dr. phil. K. Wirtz, who made possible this experiment in this Institute of Neutron Physics and Reactor Engineering. The authors acknowledge the help of P. Durand and F. Merschroth in preparing the experimental apparatus and the test sections, in performing the experiments and in the calculations of the data.

REFERENCES

1. M. Dalle Donne, The development of the gas cooled fast breeder reactor, in *Beiträge zur Kerntechnik, Karl Wirtz, gewidmet zum 65. Geburtstag*, KFK 2200 (April 1975).
2. M. Dalle Donne, Wärmeübergang von rauhen Oberflächen, KFK-Bericht, Kernforschungszentrum Karlsruhe. To be published.
3. G. Melese D'Hospital, Merit index for gas-cooled reactor heat transfer, *Nucl. Sci. Engng* **50**, 83–85 (1973).
4. L. Schiller, Über den Strömungswiderstand von Rohren verschiedenen Querschnitts und Rauigkeitsgrades, *Z. Angew. Math. Mech.* **3**, 2 (1923).
5. L. Hopf, Die Messung der hydraulischen Rauigkeit, *Z. Angew. Math. Mech.* **3**, 329 (1923).
6. K. Fromm, Strömungswiderstand in rauhen Rohren, *Z. Angew. Math. Mech.* **3**, 339 (1923).
7. A. H. Gisbson, The flow of water in a corrugated pipe, *Phil. Mag.* **50**, 199–204 (1925).
8. W. Fritsch, Der Einfluß der Wandrauigkeit auf die turbulente Geschwindigkeitsverteilung in Rinnen, *Z. Angew. Math. Mech.* **8**, 199 (1928).
9. M. F. Treer, Der Widerstandsbeiwert bei turbulenten Strömungen durch rauhe Kanäle. Die Geschwindigkeitsverteilung bei geradlinigen turbulenten Strömungen durch rauhe Kanäle, *Phys. Z.* **9**, 538 und 542 (1929).
10. S. Nikuradse, Gesetzmäßigkeiten der turbulenten Strömung in glatten Rohren, *ForschHft. Ver. Dt. Ing.* 356 (1932).
11. W. Rohl, Einfluß der Wandrauigkeit auf den Wärmeübergang an Wasser, *Forsch. Geb. IngWes.* **4**, 230–237 (1933).
12. J. Nikuradse, Strömungsgesetze in rauhen Rohren, *ForschHft. Ver. Dt. Ing.* 361; NACA TM 1292 (1950).
13. H. Schlichting, Experimentelle Untersuchungen zum Rauigkeitsproblem (Experimental Investigation of the Roughness Problem), *Ing.-Arch.* **7**(1), 1–34 (1936), NACA TM 823 (1937).
14. H. Schlichting, *Boundary Layer Theory*, 4th edn. McGraw-Hill, New York (1960).
15. H. Chu and V. L. Streeter, Fluid flow and heat transfer in artificially roughened pipes, Illinois Inst. of Tech. Proc. No. 4918 (1 August 1949).
16. E. W. Sams, Experimental investigation of average heat transfer and friction coefficients for air flowing in circular tubes having square-thread-type roughness, NACA RM E 52 D 17 (1952).
17. W. Nunner, Wärmeübergang und Druckabfall in rauhen Rohren, *ForschHft. Ver. Dt. Ing.* 455 (1956); (*Aere Lib/Trans* 786) (1958).
18. D. F. Dipprey and D. H. Sabersky, Heat and momentum transfer in smooth and rough tubes at various Prandtl numbers, *Int. J. Heat Mass Transfer* **6**, 329–353 (1963).
19. W. B. Hall, Heat transfer in channels composed of rough and smooth surface, IGR-TN/W. 832 (1958).
20. D. Wilkie, Calculation of heat transfer and flow resistance of rough and smooth surfaces contained in a single passage, in *Proceedings of the 3rd International Heat Transfer Conference, Chicago*, Vol. 1, pp. 20–31. A.I.Ch.E., New York (1966).
21. D. Wilkie and S. White, Calculation of flow resistance of passages bounded by a combination of rough and smooth surface, *J. Br. Nucl. Soc.* **6**(1–4), 48–62 (1967).
22. B. Kjellström and S. Hedberg, On shear stress distribution for flow in smooth or partially rough annuli, paper presented at the E.A.E.S. Heat Transfer Symposium on Superheated Steam or Gas, Bern, Switzerland, September 1966 and Report AE-243 of AB Atomenergi (1966).
23. D. Wilkie, M. Cowin, P. Burnet and T. Bugoyne, Friction factor measurements in a rectangular channel with walls of identical and non-identical roughness, *Int. J. Heat Mass Transfer* **10**, 611–621 (1967).
24. K. Maubach and K. Rehme, Negative eddy diffusivities for asymmetric turbulent velocity profiles? *Int. J. Heat Mass Transfer* **15**, 425–432 (1971).
25. K. Rehme, Turbulente Strömung in konzentrischen Ringspalten, Habilitationsschrift Univ. Karlsruhe, KFK Bericht 2099 (1974).
26. K. Maubach, Reibungsgesetze turbulenter Strömungen in geschlossenen glatten und rauhen Kanälen von beliebigem Querschnitt, Externer Bericht INR-4/69-22, Kernforschungszentrum Karlsruhe, BRD (März 1969).
27. K. Maubach, Rough annulus pressure drop. Interpretation of experiments and recalculation for square ribs, *Int. J. Heat Mass Transfer* **15**, 2489–2498 (1972); see also: Reibungsgesetze turbulenter Strömungen, *Chemie-Ing.-Tech.* **42**(15), 995–1004 (1970).
28. M. A. P. Watson, The performance of a square rib type of heat transfer surface, CEGB RD/B/N 1738, Berkeley Nuclear Laboratories (1970).
29. D. Wilkie, Calculation of heat transfer and flow resistance of rough and smooth surfaces contained in a single

- passage, paper presented at the E.A.E.S. Heat Transfer Symposium on Superheated Steam or Gas, Bern, Switzerland (September 1966).
30. M. Dalle Donne and E. Meerwald, Heat transfer from surface roughened by thread-type ribs at high temperatures, in Proceedings of the 1970 Heat Transfer and Fluid Mechanics Institute, Stanford Univ. Press, Stanford, Calif., June (1970); see also "Zürich Club" Gas Cooled Fast Reactor Heat Transfer Meeting, Würenlingen, Switzerland.
 31. E. Meerwald, Druckverlust und Wärmeübergang an glatten und rauhen Flächen bei hohen Temperaturen und turbulenter Strömung und deren Darstellung durch universelle Gesetze, Externer Bericht INR 4/71-29, Kernforsch. Zentr. Karlsruhe (1971).
 32. C. Warburton and M. A. M. Pirie, An improved method for analysing heat transfer and pressure drop tests on roughened rods in smooth channels, CEGB RD/B/N 2621, Berkeley Nuclear Laboratories (1973).
 33. J. B. Drew, E. C. Koo and W. M. McAdams, The friction factor for clean round pipes, *Trans. Am. Inst. Chem. Engrs* **28**, 56-72 (1932).
 34. K. Hanjalic and B. E. Launder, Fully developed flow in rectangular ducts of non-uniform surface texture. Part 1: An experimental investigation, Imperial College, Dept. of Mech. Eng. TWF/TN/48 (1968).
 35. C. J. Lawn and M. J. Hamlin, Velocity measurements in roughened annuli, CEGB RD/B/N 1278, Berkeley Nuclear Laboratories (1969).
 36. M. J. Stephens, Investigations of flow in a concentric annulus with smooth outer wall and rough inner wall, CEGB RD/B/N 1535, Berkeley Nuclear Laboratories (1970).
 37. C. J. Lee, Investigation of flow parameters for a series of concentric rough pin and smooth channel assemblies, CEGB RD/B/N 2404, Berkeley Nuclear Laboratories (1972).
 38. M. A. M. Pirie, Heat transfer and pressure drop tests on multistart ribbed surfaces covering the rib angle range 0 to 60°, CEGB RD/B/N 2760, Berkeley Nuclear Laboratories (1974).
 39. C. Warburton, The interpretation of tests on roughened pins in rough channels and the prediction of cluster pressure drop from single-pin data, CEGB RD/B/N 2930, Berkeley Nuclear Laboratories (1974).
 40. M. Dalle Donne and E. Meerwald, Heat transfer and friction coefficients for turbulent flow of air in smooth annuli at high temperatures, *Int. J. Heat Mass Transfer* **16**, 787-809 (1973).
 41. D. I. Nathan and M. A. M. Pirie, On the interpretation of heat transfer and pressure drop tests on roughened rods in smooth circular channels, CEGB RD/B/N 1370, Berkeley Nuclear Laboratories (1970).
 42. C. Warburton and M. A. M. Pirie, An improved method for analyzing heat transfer and pressure drop tests on roughened rods in smooth channels, ASME Technical paper (1974). Winter Annual Meeting, New York, 74/WA/HT/56.
 43. J. T. Wilson, Private communication, UKAEA, Windscale, England (1974).
 44. R. A. Gowen and J. W. Smith, The effect of the Prandtl number on temperature profiles for heat transfer in turbulent pipe flow, *Chem. Engng Sci.* **22**, 1701-1711 (1967).
 45. L. D. Landau and E. M. Lifshitz, *Fluid Mechanics*, p. 207, Pergamon Press, Oxford (1963).
 46. D. B. Spalding, Contribution to the theory of heat transfer across a turbulent boundary layer, *Int. J. Heat Mass Transfer* **7**, 743-761 (1964).
 47. R. A. Gowen and J. W. Smith, Turbulent heat transfer from smooth and rough surfaces, *Int. J. Heat Mass Transfer* **11**, 1657-1673 (1968).
 48. H. Ludwig, Bestimmung des Verhältnisses der Austauschkoefizienten für Wärme und Impuls bei turbulenten Grenzschichten, *Z. Flugwiss.* **4**, 73-81 (1956).
 49. A. Quarmby and R. Quirk, Measurements of the radial and tangential eddy diffusivities of heat and mass in turbulent in a plain tube, *Int. J. Heat Mass Transfer* **15**, 2321 (1972).
 50. M. Dalle Donne and E. Meerwald, Heat transfer from rough surfaces latest results, ENEA Coordinating Group on Gas-Cooled Fast Reactor Development, Heat Transfer Specialist Meeting, Windscale, England (1972).
 51. M. Dalle Donne and E. Meerwald, Heat transfer and friction correlations for surfaces roughened by transversal ribs, NEA Coordinating Group on Gas Cooled Fast Reactor Development, Core Performance Specialist Meeting, Studsvik, Sweden (1973).
 52. M. Dalle Donne, Author's replies, in *Proc. Conf. High Pressure Gas as a Heat Transfer Medium*, Vol. 181, Part 31, pp. 261-262. Inst. Mech. Engrs, London (1967).
 53. W. Baumann and K. Rehme, Pressure drop performance of artificial roughness as a function of roughness geometry, NEA Coordinating Group on Gas Cooled Fast Reactor Development, Core Performance Specialist Meeting, Studsvik, Sweden (1973).
 54. W. Baumann, Pressure drop performance of artificial roughness as a function of roughness geometry, Proc. Int. Meeting Reactor Heat Transfer, ANS, KTG, BNES, Karlsruhe (October 1973).
 55. W. Baumann and K. Rehme, Geometrieabhängigkeit des Rauigkeitsparameters von Rechteckrauhigkeiten, KFK Bericht 2131 (1975); see also: Friction correlations for rectangular roughnesses, *Int. J. Heat Mass Transfer* **18**, 1189-1197 (1975).
 56. M. Dalle Donne and E. Meerwald, Experimental local heat transfer and average friction coefficients for subsonic turbulent flow of air in an annulus at high temperatures, *Int. J. Heat Mass Transfer* **9**, 1361-1376 (1966).
 57. G. Varadi, Thermodynamische Stoffwerte von Luft, Report TM-1N-411 des Eidgenössischen Instituts für Reaktorforschung, Würenlingen, Schweiz (1969).
 58. R. L. Webb, Turbulent heat transfer in tubes having two dimensional roughness, including the effect of Prandtl number, Ph.D. Thesis, University of Minnesota (1969).
 59. M. Dalle Donne and F. H. Bowditch, Experimental local heat transfer and friction coefficients for subsonic laminar, transitional and turbulent flow of air or helium in a tube at high temperatures, Dragon Project Report 184, A.E.E. Winfrith, Dorset, England (April 1963).
 60. W. Tiedt, Berechnung des laminaren und turbulenten Reibungswiderstandes konzentrischer und exzentrischer Ringspalte, Technischer Bericht Nr. 4, Institut für Hydraulik und Hydrologie der TH Darmstadt; see also *Chemiker Zeitung/Chemische Apparatur* 90. Jahrgang (1966) 91. Jahrgang (1967).
 61. R. L. Webb, E. R. G. Eckert and R. J. Goldstein, Heat transfer and friction in tubes with repeated-rib roughness, *Int. J. Heat Mass Transfer* **14**, 601-617 (1971).
 62. H. Moebius, Experimentelle Untersuchung des Widerstandes und der Geschwindigkeitsverteilung in Rohren mit regelmäßig angeordneten Rauigkeiten bei turbulenter Strömung, *Phys. Z.* **41**, 202-225 (1940).
 63. R. Koch, Druckverlust und Wärmeübergang bei verwirbelter Strömung, *ForschHft. Ver. Dt. Ing.* **469**, Series B, **24**, 1-44 (1958).
 64. O. S. Fedynskii, Intensification of heat transfer to water in annular channel, *Sb. Statei "Problemi Energetiki" Energ. Inst. Akad. Nauk USSR* **53** (1959); [AEC-TR-4511-1962].
 65. A. Draycott and K. R. Lawther, Improvement of fuel element heat transfer by use of roughened surface and the application to a 7-rod cluster, in *Int. Dev. Heat Transfer*, Part III, pp. 543-52. ASME, New York (1961).
 66. E. Skupinski, Wärmeübergang und Druckverlust bei künstlicher Verwirbelung und künstlicher Wandrauhigkeiten, Diss. Techn. Hochschule Aachen (1961).

67. D. W. Savage and J. E. Myers, The effect of artificial surface roughness on heat and momentum transfer, *A.I.Ch.E. JI* **9**, 694–702 (1963).
68. N. Sheriff, P. Gumley and J. France, Heat transfer characteristics of roughened surfaces, UKAEA, TRG Report 447(R) (1963).
69. I. Gargaud and G. Paumard, Amélioration du transfert de chaleur par l'emploi de surfaces corruguées, CEA-R-2464 (1964).
70. F. A. Massey, Heat transfer and flow in annuli having artificially roughened inner surfaces. Ph.D. Thesis, Univ. of Wisc. (1966).
71. B. Kjellström and A. E. Larsson, Improvement of reactor fuel element heat transfer by surface roughness, AE-271 (1967).
72. G. Feurstein and G. Rampf, Der Einfluß rechteckiger Rauigkeiten auf den Wärmeübergang und den Druckabfall in turbulenter Ringspaltströmung, *Wärme- und Stoffübertragung* **2**(1), 19–30 (1969).
73. B. Kjellström, Influence of surface roughness on heat transfer and pressure drop in turbulent flow. Parts 1-2, AB Atomenergi, Sweden, AE-RTL-819 (1965).
74. N. Kattchee and W. V. Mackewicz, Effects of boundary layer turbulence promoters on the local film coefficients of ML-1 fuel elements, *Nucl. Sci. Engng* **16**, 31–38 (1963).
75. F. Williams and J. Watts, The development of rough surfaces with improved heat transfer performance and a study of the mechanisms involved, in *Proceedings of the Fourth International Heat Transfer Conference Paris—Versailles*, Vol. 2, Paper FC5.5, Elsevier, Amsterdam (1970).
76. H. M. Morris, Flow in rough conduits, *Trans. Am. Soc. Civ. Engrs* **120**, 373–410 (1955).
77. P. L. Mantle, A. R. Freeman and J. Watts, Conductivity effects on ribbed surface heat transfer, *Int. J. Heat Mass Transfer* **14**, 1825–1834 (1971).
78. M. Dalle Donne, J. Marek, A. Martelli and K. Rehme, Forced convection heat transfer in a roughened 12 rod bundle, NEA Coordinating Group on Gas Cooled Fast Reactor Development, Heat Transfer Specialist Meeting, Petten (17–19 September 1975).
79. V. Walker, L. White and P. Burnett, Forced convection heat transfer for parallel flow through a roughened rod cluster, *Int. J. Heat Mass Transfer* **15**, 403–424 (March 1972).

CONVECTION THERMIQUE TURBULENTE A PARTIR DE SURFACES RENDUES RUGUEUSES PAR DES NERVURES RECTANGULAIRES A DEUX DIMENSIONS

Résumé—La rugosité artificielle est fréquemment utilisée dans les réacteurs nucléaires pour améliorer la performance thermique des éléments de combustible. Bien que ces éléments soient constitués de faisceaux de barres, les expériences visant à la mesure des coefficients du transfert de chaleur et de frottement de la rugosité s'effectuent sur une barre unique entourée d'un tube lisse. Ce mémoire décrit une nouvelle méthode de transformation permettant d'acquérir des données valables pour les éléments de combustible du réacteur moyennant des expériences faites dans cet espace annulaire. Des mesures nouvelles du coefficient de frottement ont été conduites pour dix barres rugueuses avec des nervures rectangulaires à deux dimensions. Pour chaque barre quatre mesures ont été effectuées, chaque fois avec un tube lisse extérieur différent. Les mesures des coefficients de transfert de chaleur concernent deux de ces barres. Pour chacune de ces deux barres deux mesures ont été faites, chaque fois avec un tube lisse extérieur différent. Les données sur le frottement ainsi que sur le transfert de chaleur, transformées à l'aide de la méthode décrite, ont été condensées par des formules simples. Celles-ci sont appliquées dans ce mémoire à un exemple caractéristique pour l'élément de combustible d'un réacteur rapide refroidi au gaz.

TURBULENTE KONVEKTIVE WÄRMEÜBERTRAGUNG VON OBERFLÄCHEN MIT ZWEIDIMENSIONALEN RECHTECKIGEN RAUHIGKEITSRIPPEN

Zusammenfassung—Durch künstliche Rauigkeit kann in Kernreaktoren die Wärmeübertragungsfähigkeit der Brennelemente verbessert werden. Obwohl die Brennelemente aus Stabbindeln bestehen, werden die Experimente zur Messung der Wärmeübertragungs- und Reibungskoeffizienten der Rauigkeiten an Einzelstäben in glatten Röhren durchgeführt. Der Beitrag beschreibt eine neue Transformationsmethode, mit der Daten für Reaktor Brennelemente aus diesen Versuchen im Ringspalt erzielt werden können. Reibungsbeiwerte wurden an zehn verschiedenen rauhen Stäben mit rechteckigen Rippen in jeweils vier verschiedenen glatten Außenrohren und Wärmeübergangskoeffizienten an zwei dieser rauhen Stäbe in jeweils zwei der glatten Außenrohre gemessen. Die mit Hilfe der vorgestellten Methode transformierten Reibungs- und Wärmeübertragungswerte werden durch einfache Gleichungen beschrieben. Diese Gleichungen werden auf einen Fall angewandt, der für ein Brenn-element eines gasgekühlten schnellen Reaktors typisch ist.

ТУРБУЛЕНТНЫЙ КОНВЕКТИВНЫЙ ПЕРЕНОС ТЕПЛА ОТ ПОВЕРХНОСТЕЙ С ШЕРОХОВАТОСТЬЮ В ВИДЕ ПЛОСКИХ ПРЯМОУГОЛЬНЫХ РЕБЕР

Аннотация—Искусственная шероховатость часто используется для улучшения эффективности ТВЭЛов ядерных реакторов. Хотя ТВЭЛы собираются из пучков стержней, опыты по измерению коэффициентов теплоотдачи и трения шероховатых поверхностей проводились на единичных стержнях, помещенных в гладкостенные трубы. В статье рассматривается новый метод преобразования данных, полученных для единичного стержня в трубе, применительно к ТВЭЛам ядерных реакторов. Приводятся новые экспериментальные данные по трению для десяти стержней с различной искусственно нанесенной шероховатостью в виде плоских прямоугольных ребер, каждый из которых помещался в четыре различные гладкостенные трубы. Для двух из этих стержней в двух различных трубах приведены данные по теплоотдаче. Для обобщения данных по трению и теплоотдаче, преобразованных с помощью предложенного метода, используются простые формулы, применение которых показано на примере ТВЭЛа реактора на быстрых нейтронах с газовым охлаждением.